New Tools to Understand Mechanisms of Nutrient Transfer from Plants to Biotrophic Pathogens

Kasia Dinkeloo

Dissertation submitted to the faculty of the Virginia Polytechnic Institute and State University in partial fulfillment of the requirements for the degree of

Doctor of Philosophy
In
Plant Pathology, Physiology, and Weed Science

Guillaume Pilot and John McDowell, Committee Chairs
Bingyu Zhao
David Haak

26 July 2018

Key Words: Plant-Pathogen Interactions, Translatome, Transcriptomics, RNA, Methods, TRAP, GFP

New Tools to Understand Mechanisms of Nutrient Transfer from Plants to Biotrophic Pathogens

Kasia Dinkeloo

Academic Abstract

The interaction between *Arabidopsis* and its natural downy mildew pathogen, *Hyaloperonospora arabidopsidis* (*Hpa*), provides a model for understanding how oomycetes colonize plants. *Hpa* is a model organism for many highly destructive oomycete pathogens and transcriptomics of this interaction have been well-documented. However, the material in these studies has been derived from infected leaves that contain a mix of pathogen-proximal and pathogen-distal plant cells. The most direct interactions between *Arabidopsis* and *Hyaloperonospora arabidopsidis* occur in haustoriated cells- where the pathogen can secrete effectors and acquire nutrients needed for successful colonization and reproduction. These cells are difficult to isolate due to their limited number and ephemeral nature. I have developed a method to isolate the translatome (i.e., mRNAs associated with ribosomes) of pathogen-proximal cells. This method utilizes translating ribosome immuno-purification technology (TRAP), regulated by both pathogen-responsive and tissue-specific promoters, to isolate mRNAs that are being translated in pathogen-proximal cells. Compared to "bulk" transcriptomics of material isolated from homogenized leaves, this method will enrich for transcripts that are differentially expressed, and translated, in pathogen-proximal cells. From this method, RNA was isolated in amount and quality sufficient for sequencing. This sequencing data will enable the discovery of plant genes that may be manipulated by the pathogen to suppress defense responses and extract nutrients.

New Tools to Understand Mechanisms of Nutrient Transfer from Plants to Biotrophic Pathogens

Kasia Dinkeloo

General Audience Abstract

The interactions between plants and the pathogens that feed on them are complex and at times difficult to study. Among the many different types of plant pathogens, oomycetes (a class of fungus-like organisms) are especially destructive. Using *Arabidopsis* and its natural downy mildew pathogen, *Hyaloperonospora arabidopsidis* (*Hpa*) as model for understanding how oomycetes colonize plants, I hope to learn more about plant-pathogen interactions. *Hpa* is a model organism for many highly destructive oomycete pathogens and several aspects of this interaction have been well-documented. However, the material in these studies has been derived from infected leaves that contain a mix of plant cells that are both in direct contact with the pathogen, or from uninfected areas of the plant. The most direct interactions between *Arabidopsis* and *Hpa* occur in cells that have been invaginated with a pathogen feeding structure called a haustorium. These cells are difficult to isolate due to their limited number and ephemeral nature. I have developed a method to isolate the translatome (i.e., mRNAs that are being translated by and are associated with ribosomes) of pathogen-proximal cells. This method utilizes translating ribosome immuno-purification technology (TRAP), regulated by both pathogen-responsive and tissue-specific promoters, to isolate mRNAs that are being translated in pathogen-proximal cells. Compared to "bulk" transcriptomics of material isolated from homogenized leaves, this method will enrich for transcripts that are differentially expressed, and translated, in pathogen-proximal cells. From this method, RNA was isolated in amount and quality sufficient for sequencing. This sequencing data will enable the discovery of plant genes that may be manipulated by the pathogen to suppress defense responses and extract nutrients.

Acknowledgements

I would like to first acknowledge my primary advisors, Dr. Guillaume Pilot and Dr. John McDowell. They have given me patient guidance, constant support, and excellent mentorship over the past five years. I would like to especially thank Guillaume for the hands-on training he provided during my first year of my PhD, the time he set aside for weekly meetings, and the copious amounts of editing and feedback he provided for abstracts, applications, posters, and presentations. I would like to thank John for his grounded sense of perspective and encouragement during difficult moments of research.

In addition, I would like to thank my committee members, Dr. David Haak and Dr. Bingyu Zhao. I am grateful for your guidance and input throughout this project. Thank you for making time for our meetings and signing and filling out the many forms at come with being a committee member. Thank you, David, for all of your help as both and instructor in a formal course, as well as a mentor/committee member as it pertained to submitting and handling my RNA sequencing data. I am incredibly grateful to have your input and expertise on this part of my project.

I was very fortunate to not only have wonderful co-advisors and committee members, but also to be a part of two wonderful lab groups. I would like to recognize my lab mates past and present: John Herlihy, Wei Wang, Dr. Colin Davis, Dr. Shi Yu, Dr. Chengsong Zhao, Dr. Cindy Denbow, Dr. Joel Shuman, and Brett Shelley. It was truly a pleasure to work with such a great group of individuals. I would like to distinctly thank Unnati Sonawala and Shelton Boyd, with whom I have shared so many long days, lab meetings, conference trips, joys and sorrows of research, and all of the little things that make graduate school an experience unlike any other. I feel deeply fortunate to have had partners in science like them. I would also like to especially thank Erik Leith and Zoe Pelley, two undergraduate students that I had the pleasure of mentoring. I appreciate their work ethic, resilience, and optimism as young scientists. Thank you for allowing me to grow as a mentor through your research experiences.

I am incredibly thankful to my department of Plant Pathology, Physiology, and Weed Science, as well as the Translation Plant Science program for fostering an inclusive community of scientists. I feel that my graduate learning experience was greatly enriched due to the tight group of supportive faculty and students. I loved being a part of a passionate and fun department, and thoroughly enjoyed the graduate student community fostered by both programs. I am grateful to TPS for their funding opportunities, allowing me to travel to Munich, Germany and Asilomar, California for conferences that I may not have been able to attend otherwise.

In all things that I do, I am thankful for my family. I would like to thank my parents, Dirk Dinkeloo and Erin Jacob, for unconditional support and enthusiasm at all stages of my PhD (and all stages leading up to it as well). I would like to thank my brothers, Arie and Eero Dinkeloo, for their support as well. My brothers serve as constant sources of energy, positivity, and humor when I need it most. I would like to thank my close friends Brianne Richardson, Daniel Surinach, Kelsey Sum, Alexa Grant, and Brian Sever for being voices of encouragement, love, and reason. I would like to especially thank Caitlin Worsham and her family for making a new place feel like home. I am grateful to Caitlin for her friendship and support from the very first months of my PhD to its completion.

Table of Contents

LIST OF TABLES

LIST OF FIGURES

CHAPTER I

Introduction

Plant Pathogens and Their Importance

It has been established that a majority of the world's calories come from food crops. The human population (and the demand for meat/livestock) is increasing, yet there is a continual decrease in the amount of arable land for food production [1]. As such, we must direct our time and resources to studies that will allow for an increase of food production on less available land. To do this, we must make plants more productive, and provide more effective means of protecting them from pathogens and pests that destroy crop yields. Plant pathogens carry a huge economic impact. An example of this impact can be seen in the costs of the oomycete pathogen responsible for the Irish potato famine, *Phytophthora infestans*. In the United States alone, *P.infestans* control methods cost an estimated $77 million for fungicides, and an additional $210.7 million in lost revenue for growers [2]. If left uncontrolled or sometimes even in spite of control measures, certain plant pathogens can cause complete yield loss [3]. This is not only a loss of food/product, but also a waste of all the resources committed to the growth of the plants such as water, fertilizer, and fossil fuels. Protecting and improving plants is an important societal endeavor for the survival of our population, and the health of the planet. This dissertation reports the development of new tools to facilitate basic research that will lay a foundation for new methods to reduce losses to crop diseases.

Current strategies for disease control

Currently, several strategies exist to minimize or combat losses from plant pathogens: chemical control in the form of pesticides, biological control in the form of beneficial microbes or insects, and plant-based resistance from selective breeding and genetic engineering of resistance genes (R-genes). In these cases, however, there is always concern for the durability or longevity of effectiveness in the field. Rationales for these concerns can be found in the instance of resistance to fungicides, breakdowns of varietal resistance (especially in the case of major resistance genes), or the inconsistency found with biological control in varying field conditions [4]. The breakdown of resistance is costly both from the perspectives of both product loss (of crops) and product development (of the control strategy). As such, novel methods or aspects of resistance are incredibly important. In order to develop such novel methods for pathogen control, the interactions between plants and pathogens must be studied in new ways.

Obligate Biotrophs

Plant pathogens follow several different lifestyles that are categorized through the pathogens' interactions with the host plant. Biotrophs extract nutrients from living plant cells and do not kill their host. Contrastingly, necrotrophs kill host tissue to feed from it, while hemibiotrophs initially employ a biotrophic lifestyle, but switch to necrotrophy to complete their lifecycle. Obligate biotrophic organisms require a living host for their establishment, growth, and reproduction, and cannot be cultured apart from their hosts. Obligate biotrophs are found in both fungi and oomycetes and can grow as beneficial partners, asymptomatic companions, and even highly destructive plant pathogens [5].

Hyaloperonospora arabidopsidis (*Hpa*) is an obligate biotrophic parasite that causes downy mildew on Arabidopsis. *Hpa* belongs to the oomycetes: eukaryotic organisms similar to fungi but are more closely related to brown algae or diatoms [6]. Although many oomycetes may look like fungi, they differ in the composition of their cell wall (very little to no chitin) and their hyphae lack septa (meaning they are coenocytic)[6]. Beyond appearance, oomycetes also differ from fungi in some biochemical pathways, for example they create unique signaling compounds and they have more diverse fatty acid profiles [7]. Thus, phytopathogenic oomycetes and fungi have evolved convergently to colonize plant hosts.

As an obligate pathogen that has co-evolved with Arabidopsis, *Hpa*'s life cycle is dependent on its living host. The asexual lifecycle begins when a spore comes into contact with the surface of a leaf. The spore germinates, produces an appressorium and penetration hypha, and then penetrates the leaf between two epidermal cells. As hyphae grow between cells in the leaf, haustoria are formed and invaginate mesophyll cells so that the pathogen can take up nutrients and secrete effectors. *Hpa* grows throughout the extracellular space in the leaf and makes sporangiophores that grow out of stomata and produce proliferous amounts of asexual spores. These spores can then re-start the life cycle on new hosts. *Hpa* also produces sexual spores called oospores. These are produced within the leaf and can be employed as overwintering structures, surviving in soil or leaf debris until they come into contact with a new host plant [6]. This lifecycle is depicted in figure 1.

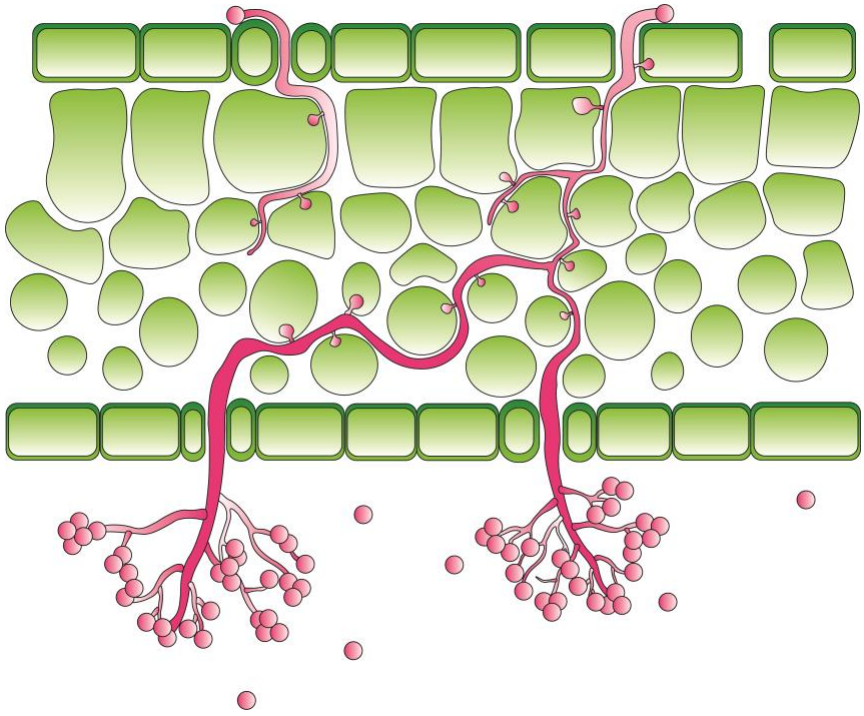

Figure 1. Diagram of *Hyaloperonospora arabidopsidis* growth through an Arabidopsis leaf section. Spores germinate on the adaxial leaf surface (a), penetrate the epidermis and growth intracellularly, producing haustoria that invaginate mesophyll cells (b). As the infection progresses, hyphae give rise sporangiophores that protrude from the abaxial leaf surface and produce many spores for new infection (c).

The haustorium is a specialized hypha that invaginates a plant cell, allowing the pathogen to sequester nutrients and secrete effectors (Figure 2). The insertion of the haustorium does break the host cell's plasma membrane, but the insertion also results in the formation of an extrahaustorial membrane by the host cell [8]. In addition to the membrane formation, components of the host cells such as ER, Golgi bodies, and nucleus move towards the penetration site [9]. As such, the haustorium serves as the point of communication between the pathogen and its host. Cells that are in association with haustoria are defense-compromised due to the interactions between effectors and host proteins that regulate immunity [10]. Despite their importance as sites of direct plant-pathogen contact and communication, the molecular events that occur specifically in haustoriated cells remain to be defined.

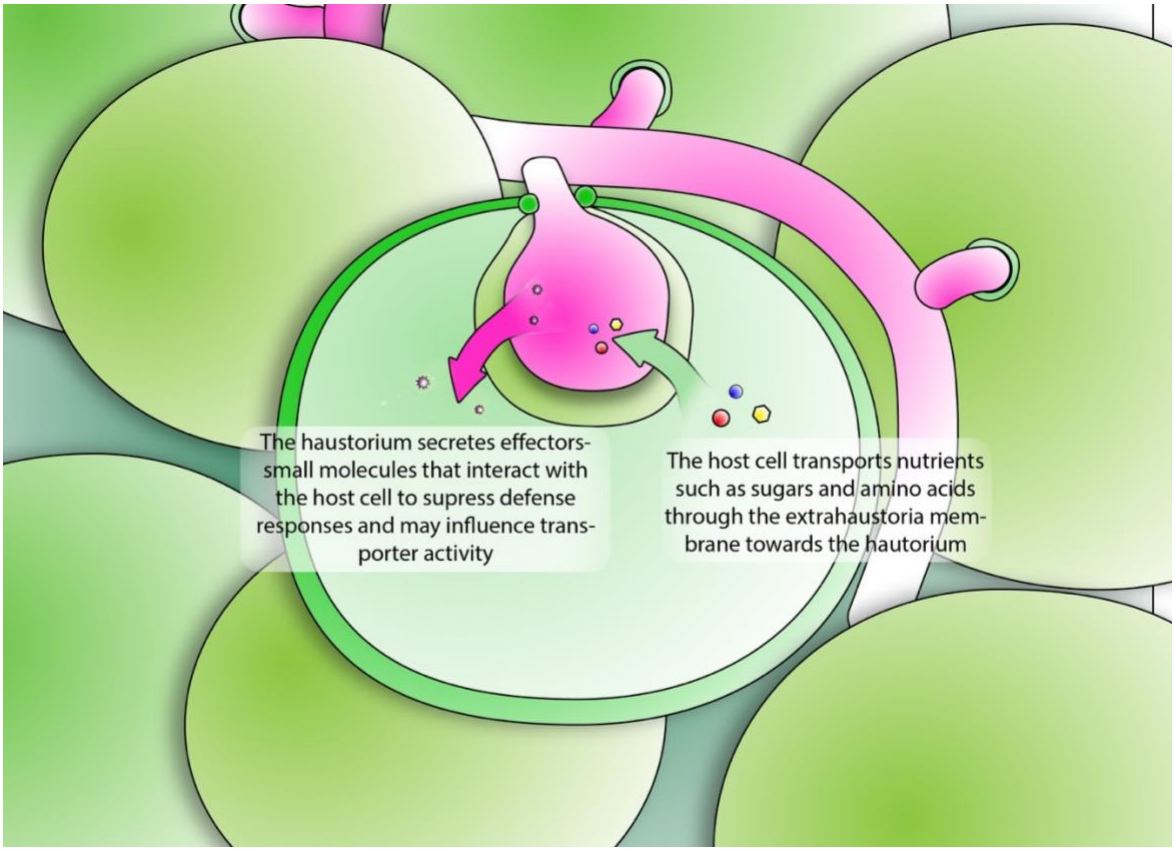

Figure 2. Diagram of a haustorium invaginating a mesophyll cell. The haustorium (in pink) is kept separate from the plant cell by the extrahaustorial membrane. Interactions between the plant cell and pathogen occur via secreted molecules across the extrahaustorial matrix.

Nutrient transporters as targets for engineering durable resistance

Durable resistance is defined as resistance that remains effective when employed widely in environments that favor disease development, and is an incredibly valuable resource for breeding [11]. Classically, many of the resistance targets have been defense-associated and fall into the category of gene-for gene resistance. Manipulation of host defenses has been advantageous in the fight against pathogens, but a breakdown of resistance usually occurs due to selective pressure and the highly-adaptable nature of pathogen populations. A potential novel set of targets for durable resistance are plant nutrient transporters that certain pathogens require for feeding and development. These genes,

such as amino acid or sugar transporters, could be altered in their expression, localization, or molecular function to become inaccessible to the pathogen, allowing for resistance via starvation. This resistance may be more durable than host-defense manipulation strategies due to the pathogen being unable to reproduce after spending its stored resources on penetration and initial growth within the host. An example of this resistance can be found in the interactions between Arabidopsis and certain bacteria, where the altered expression of an Arabidopsis monosaccharide transporter (STP13) depletes sugars from the apoplasm during infection decreasing its availability for the pathogen [12]. Currently, little is known about how plant pathogens extract nutrients from their hosts. This is particularly true for oomycetes. However, background information on other pathogens that have been shown to induce nutrient transport from their hosts can be used as a foundation to hypothesize that *Hpa* may do the same.

Functional linkages between plant nutrient transporters and pathogen nutrient acquisition

The attention surrounding amino acid transporters is due to the fact that *Hpa* lacks genes for nitrate and nitrite reductases, a nitrate transporter, and sulfite reductase. These genes, and the associated pathways for assimilation of inorganic nitrogen and sulfur, are evolutionarily conserved in oomycetes and fungi that are non-obligate. However, one or more of these genes/pathways have been deleted in all oomycete or fungal lineages that have evolved to an obligate lifestyle [13, 14]. Collectively, the lack of these genes indicates that these organisms depend on sources of reduced nitrogen and sulfur, most likely in the form of amino acids.

Other examples of obligate biotrophs with altered metabolism pathways include both oomycetes and fungi. *Albugo laibachii* (an oomycete) evolved biotrophy independently of *Hpa*. *A. laibachii* has lost the whole molybdopterin (a cofactor required for nitrate reductase and sulfite oxidase function) biosynthesis pathway in addition to the genes observed to be missing from *Hpa* [15]. *Golovinomyces orontii* (a powdery mildew fungus) lacks the thiamine biosynthetic pathway. In the oomycetes, all haustorium-forming species have lost the thiamine biosynthetic pathway leading to the inference that oomycetes obtain thiamine from the host as well [16].

Oomycete pathogen feeding structures are surrounded by a novel, host-produced membrane. It has also been shown that these pathogens need certain nutrients from the host (sugars, nitrogen-possibly in the form of amino acids). However, evidence that is there amino acid transport occurring at the host/pathogen interface has only been shown in select studies conducted on rust pathogens.

It has been shown that activity of H^+-ATPase isolated from haustorial plasma membranes of *Uromyces fabae* strongly increased compared to other fungal structures. H^+-ATPase creates proton-motive force that may provide energy for transport processes across haustorial membranes, supported by the fact that in both plants and fungi, nutrient uptake is driven mostly by an H^+ electrochemical gradient [17]. In addition to the increase of H^+-ATPase activity, three fungal amino acid transporters (Uf-AAT1, Uf-AAT2, and Uf-AAT3) are highly expressed exclusively in haustoria. In accordance with other obligate biotrophs, *U.fabae* also lacks the nitrate assimilation pathway. However, genes encoding enzymes for amino acid biosynthesis and metabolism have been identified, suggesting that amino acids taken up from the host can be metabolized [17].

Uptake of essential elements is an important component of pathogen feeding, but other nutrients are required for life. As the main product of photosynthesis, sugars are a valuable resource for both the plant and pathogens [18]. In the plant, sugars are typically transported symplasmically from cell to cell. When apoplasmic transport is required, sucrose transporters (SUTs) translocate sugars into the cell, and SWEETs (another class of sugar transporters) secrete sucrose out of the cell [19]. SWEET transporters are of special interest to pathologists because their expression of some members can be induced by bacterial pathogens [20].

Bacterial pathogens are not alone in targeting SWEET transporters. The fungal powdery mildew pathogen *Golovinomyces cichoracearum* has been shown to induce a different set of AtSWEET mRNAs, most prominently AtSWEET12 [20]. *SWEET*2 is also a target- its root expression was induced more than 10-fold during *Pythium sp*. infection. Importantly, *sweet2* mutants were more susceptible to the oomycete, showing impaired growth after infection [21].

Collectively, the information gathered from different plant pathogens points towards the hypothesis that oomycetes employ a "metabolic colonization" of infected plant host cells- meaning that these pathogens alter the host metabolism to fit their nutrient requirements [22]. With so much left to be discovered, there is a strong need to fill the gap in knowledge through the development of technology that gives us access to the wealth of information that this aspect of plant-pathogen interaction can provide.

Limitations of current technology for the study of the interaction between Arabidopsis and *Hpa*

Transcriptomics are a powerful tool for gene analysis and discovery. To identify novel susceptibility genes from our model pathosystem, there are several obstacles that must be overcome. For example, only a small percentage of plant cells are in direct contact with the pathogen's haustoria (figure 3). As such, transcriptome data from infected whole leaves are most likely "noisy", in that a majority of the genes showing change in expression are expected to be dedicated to defense responses, and changes in gene expression that occur in haustoriated cells could be lost due the "averaging" effect that results from homogenization of leaves in which the majority of cells are pathogen-distal.

Figure 3. Trypan stain of Arabidopsis leaves. Trypan staining shows pathogen hyphae and haustoria in an infected 3-week-old leaf. Although heavily colonized, a majority of mesophyll cells are not in contact with haustoria. Trypan blue also lightly stains vascular tissue, as seen in the noninfected sample.

Several techniques to isolate subpopulations of cells exist. One example is laser-capture microdissection (LCM), which depends upon direct microscopic visualization to directly harvest or enrich for specific cells from a complex sample [33]. Another technique is fluorescence-activated cell sorting (FACS)- a type of flow cytometry that separates labeled cells (e.g., expressing a pathogen-inducible GFP transgene) based on analysis of light scattering and fluorescent characteristics [33, 34]. These techniques, however, are generally expensive, technically difficult due to impaired visualization, and are subject to technical artifacts from the extraction techniques [35, 36]. An ideal system to study the sub-population of haustoriated cells compared with the whole in Arabidopsis wouldn't require protoplasting, embedding, or dissection, would be easily scalable, customizable, and preferably inexpensive (in the sense that it does not require expensive or unusual equipment). Based on these requirements, a my dissertation project was to develop Translating Ribosome Affinity Purification as a system for cell-specific transcript profiling in the Arabidopsis-*Hpa* interaction.

Translating Ribosome Affinity Purification

Translating ribosome affinity purification (TRAP) was pioneered as a technique to reproducibly isolate currently-translated mRNAs from genetically-defined cell sets in mice [37]. This technique was based on creating transgenic plants expressing a ribosomal protein with a purification tag and expressing this tagged ribosomal protein gene under the control of a cell-type specific or condition dependent promoter (figure 4). Tissue is collected under the condition of study and total proteins are extracted. Then, the tagged ribosomes are purified from total protein extract via immunoprecipitation with an antibody against the tag fused to the transgenic ribosomal protein [38, 39]. This approach will enrich for ribosomes from the cell type of interest because the tagged ribosomal protein transgene is

expressed only in the specific cell type(s) or conditions in which the transgene's promoter is active. RNA can then be isolated from the immunopurified ribosomes and subjected to RNA sequencing. In this way, it is possible to achieve cell type-specific transcriptomics without purifying specific cell types.

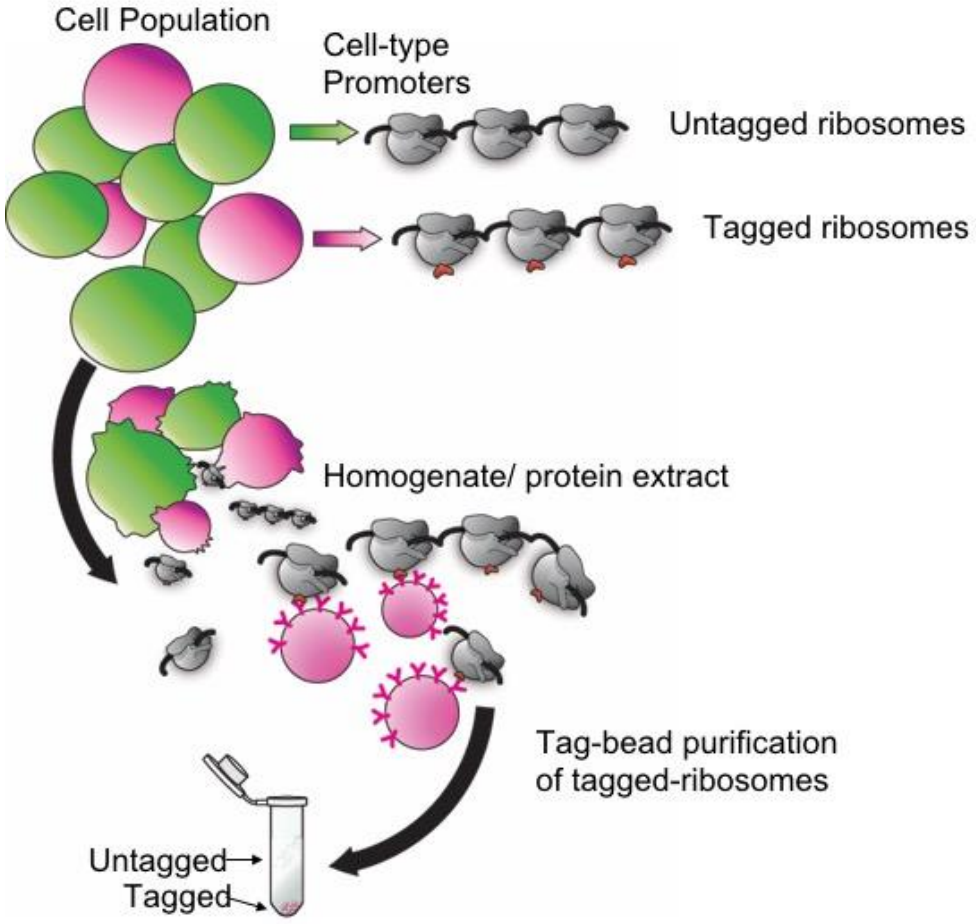

Figure 4. Illustration of Translating Ribosome Affinity Purification. Tagged ribosomes are expressed under the control of a cell type-specific promoter (magenta). Tissues are homogenized and proteins are extracted. The homogenate is added to antibody beads, so that only tagged ribosomes are immunopurified from bulk tissues.

Another advantage of TRAP is that It enriches for transcripts that are actively translated. Conventional transcriptomics captures total mRNA, including those mRNAs that are not being translated at the time of isolation. Thus, this approach does not capture the control that an organism can exert during translation [40]. TRAP provides researchers with access to the cell's translatome- the collection of mRNAs that are currently associated with and being translated by polysomes (groups of ribosomes translating the same mRNA) or single ribosomes. These mRNAs (sometimes referred to as ribosome-nascent chain complex bound, or RNC-mRNAs) stand as an independent predictor of (and more closely correlated to) protein synthesis than does information from total mRNA/transcriptome alone [41].

The differences in analysis of gene expression between what is portrayed from the transcriptome versus the translatome have been described in several organisms and can be significantly influenced by the conditions placed upon a given organism. For example, in yeast cells subjected to

harsh stresses (that would stop cell growth) changes in transcriptome were correlated with changes in the translatome. However, when the cells were subjected to more mild stresses, gene expression was mostly regulated at the translational level via the regulation of association of mRNAs with ribosomes [42]. As for plant-pathogen interactions, a study of Arabidopsis responding to the bacterial effector AvrRpm1 showed significant translational reprogramming upon activation of the resistance gene RPM1 that recognizes avrRpm1 [43]. Specifically, there was a difference in the translational status of a number of genes that would not have been otherwise predicted from their total abundance. Reverse genetics of selected candidates from these data revealed new genes that play a role in immunity to bacteria and also to *Hpa*. Thus, we expect that comparison of transcriptome and translatome in *Hpa*-infected tissue will reveal new molecular aspects of the Arabidopsis-*Hpa* interaction that would not be evident with transcriptomic data alone.

Outside of the comparisons that are drawn between a cell type's transcriptome and translatome, TRAP allows for the purification of the translatome from specific cells, that can then be compared to the translatome or transcriptome of the varied cell types that make the whole of an organism. In plants, TRAP has been used to study the translational response of different cell types to environmental stresses such as hypoxia (from which it was determined that different cell sets had distinct translatomes but responded uniformly by promoting translation of mRNAs that allow for acclimation) [44]. Analyzing a seedling's transcriptome under these conditions would mostly likely lead to the loss of the specific responses within the "noise" of the rest of the transcriptome. In this project, the TRAP system will be modified to capture the translatome of haustoriated cells, whose cellular responses may have been otherwise lost in the "whole leaf" response to the pathogen that has been collected from in previous transcript profiling experiments.

Project Goals

The goals for this dissertation were as follows: First, create a new TRAP system in Arabidopsis for the collection of genetic information from pathogen-proximal, pathogen-distal, and whole-leaf cell sets. Second, RNA sequencing of the genetic information will be analyzed in the context of nutrient transport between host and pathogen. This analysis will yield candidate transporters to be used for further experiments/validation. Lastly, an assay to track the transfer of labeled amino acids from host to pathogen was developed quantify the transfer of nutrients between the plant and pathogen for analysis of transporter mutants.

CHAPTER II

Designing the TRAP technology

What do we need from our TRAP technology?

In classical TRAP systems, a tagged ribosomal protein gene is regulated by a cell-type or condition-dependent promoter so that the protein is present in the desired cell type or in response to a condition of interest. In the case of haustoriated cells, the pathogen is active both in a limited time frame (7 days total) and in limited number of plant cells (only those that will contain haustoria, which

increases throughout those 7 days prior to sporulation). Since the details and timing of ribosome biogenesis in plants is not completely understood and ribosomes themselves seem to be relatively stable within a cell (let alone one that may be metabolically altered during pathogen presence), it may be disadvantageous to try to express a ribosomal protein under the control of a pathogen-inducible promoter. Specifically, it is unknown how long it would take for the expressed protein to be incorporated in an active and functional ribosome, as well as have enough of these tagged ribosomes in the cell for immunopurification. Thus, we altered the design of conventional TRAP to include a split-linker protein system, in which one fragment of the split linker, containing the purification tag, is under the control of the pathogen-inducible promoter, while the ribosomal protein fused with the other half of the split protein is constitutively expressed under the control of a mesophyll-specific promoter, corresponding to the tissue type that the pathogen parasitizes (figure 5).

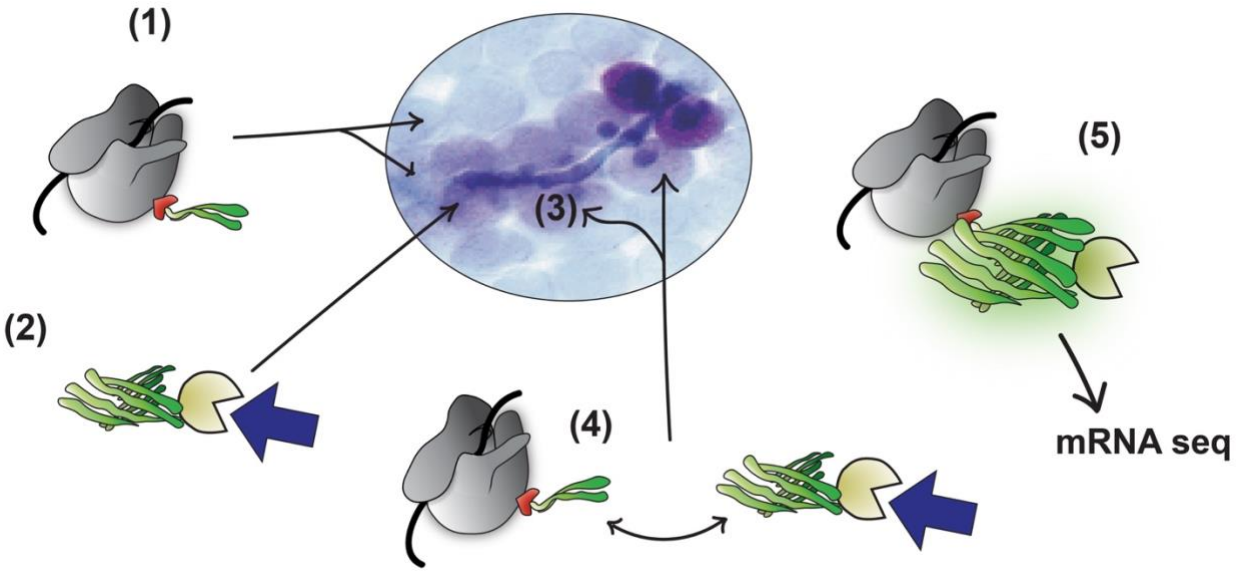

Figure 5. Modified TRAP system. (1) Ribosomes tagged with one segment of split-GFP are synthesized in all mesophyll cells. (2) The second segment of the GFP is fused to a purification tag, expressed under the control of the DMR6 promoter. (3) In cells containing haustoria, the GFP segments assemble into a functional fluorophore. (4) The re-assembly of the two segments of the GFP will link the ribosome to the purification tag. (5) This allows for purification of ribosomes (and translated mRNAs) specifically from cells that contain haustoria. DMR6pro:GUS staining image from Van Damme et al [45].

Linker protein selection

Successful immunopurification of polysomes is dependent upon on a stable and strong association of the ribosomal protein with the inducible purification tag via the linker protein. As such, it is important to select a modular protein from which two fragments can be expressed from separate genes and reconstitute in close proximity with high affinity. The ideal linker protein is small (less than 50 kDa), stable in plant cells, and readily detectable by common experimental techniques.

Green fluorescent protein (GFP) from the jellyfish *Aequorea Victoria* has been used in molecular biology as a reporter gene due to its fluorescent properties from its internal chromophore [46]. GFP is composed of 11 beta sheets that form a barrel around the chromophore; as such, it can be used as a "split" protein that will spontaneously assemble when its fragments are in close proximity to each other

[47]. In addition to its properties as a linking protein, the fluorescence is an added advantage in that we will be able to confirm activity of both genes and assembly of the respective fragments through visualization of fluoresence in the transgenic plants.

Due to issues with aggregation and mis-folding when expressed in *E.coli* and other organisms, GFP has been mutagenized to mitigate these issues. One such GFP variant is the robustly-folding "superfolder" GFP that shows fluorescence proportional to total expression [48]. The superfolder GFP is the basis for a tripartite split protein that is even further mutagenized for reconstitution and folding efficiency, and this tripartite superfolder GFP protein was selected as the protein linker for this project [49]. We made one modification to the protein by removing an 11AA long "linker" sequence between the 10^{th} and 11^{th} beta sheets, since we will not be using it in a tripartite fashion.

Promoter selection

Promoters will dictate when and where different constructs will be expressed within the plant. Promoters will be chosen for specificity to pathogen-proximal cells (in an inducible manner), non-proximal cells (also pathogen inducible), and mesophyll tissue. A promoter must also be selected which confers a strong, constitutive expression in all tissues for preliminary testing. Candidates for these promoters are outlined in Chapter IV. All constructs will contain the TMV omega translational enhancer- the 5'-leader sequence of tobacco mosaic virus (TMV) [50].

Tags, Spacers, and enhancers

In published trap protocols, a Flag-tag (DYKDDDDK) is used in conjunction with α-flag beads and for purification. A flag peptide is then used to elute the precipitated proteins from the beads. We propose to keep this purification tag due to its established effectiveness in plant protein extracts. The Flag-tag will be fused to one part of the split protein linker and controlled by the pathogen-inducible promoter. In addition, we will add a second tag to the constitutively expressed ribosomal protein. For this, we have chosen the cMyc-tag. This additional tag will be used for quality control assays in case we need to examine expression or accumulation of the ribosomal protein.

When adding modules such as epitope tags and GFP fragments to a ribosomal protein, care must be taken to ensure that these additions do not interfere with the functionality of the ribosomal complex while allowing sufficient flexibility for assembly of the split GFP and accessibility of the FLAG tag for purification. It is also possible that too much space may encourage protein cleavage of the fusion from the ribosomal complex. Therefore, we included "spacers"- small amino acid chains that sit between the different modules in our proteins to allow for natural movement.

CHAPTER III

The Map to TRAP: GenoCAD and In-Fusion cloning

After careful review of existing literature and protein databases, a set of split proteins and linkers were chosen. These fragments were then organized, in silico, into "blocks" of DNA sequence which could be ordered as synthetic double-stranded DNA from Integrated DNA Technologies. The resulting fragments, called "gBlocks" were received as dry DNA, resuspended, cloned into plasmid vectors, and used as templates for PCR for the amplification of the desired fragments, dictated by primer specificity (figure 6). These fragments were used for in-fusion cloning as described below.

GenoCAD software was used to organize and create gene fusion constructs for each of our promoter/spacer/linker combinations. GenoCAD employs the use of "grammar" such that the design process is subject to a set of rules developed by the researcher or other users in the network [51]. From this, DNA fragments and constructs were created. These constructs were saved as genbank formatted files and exported from GenoCAD for use in VectorNTI.

VectorNTI is a commercially-available software for plasmid vector design and sequence analysis. The constructs from GenoCAD were imported into this software, which was then used to manually design primers for amplification of fragments for in-fusion multiple fragment cloning. To create fragments for use in this cloning system, we designed primers with 15-20 bp overlaps (additional sequence on either side of the specific fragment) with identity to the fragments next to which the amplified fragment would anneal. In-fusion cloning uses an enzyme with 3'-5' exonuclease activity that creates overhangs from the overlapping sequences, allowing for multiple fragments to be annealed in one cloning event. Using this approach, a total 102 different DNA fragments were assembled.

These fragments were then amplified by PCR with the proofreading KOD polymerase, and gel purified for insertion into plasmid vectors. Challenges were encountered at this step when attempting to amplify and purify very large or very small fragments. For large PCR products, touchdown PCR programs were used. For small products, the challenge of gel purifying small bands was solved by increasing the content of agarose in the gel to resolve them more clearly for excision from the gel. Care was taken at this step to ensure that all fragments were purified at a high enough yield for successful cloning. The plant expression vector pPTkan4 was linearized via digestion for use with the in-fusion system. *E. coli* was transformed with the resulting constructs. DNA from these clones was sequenced to confirm polymerase fidelity and cloning accuracy.

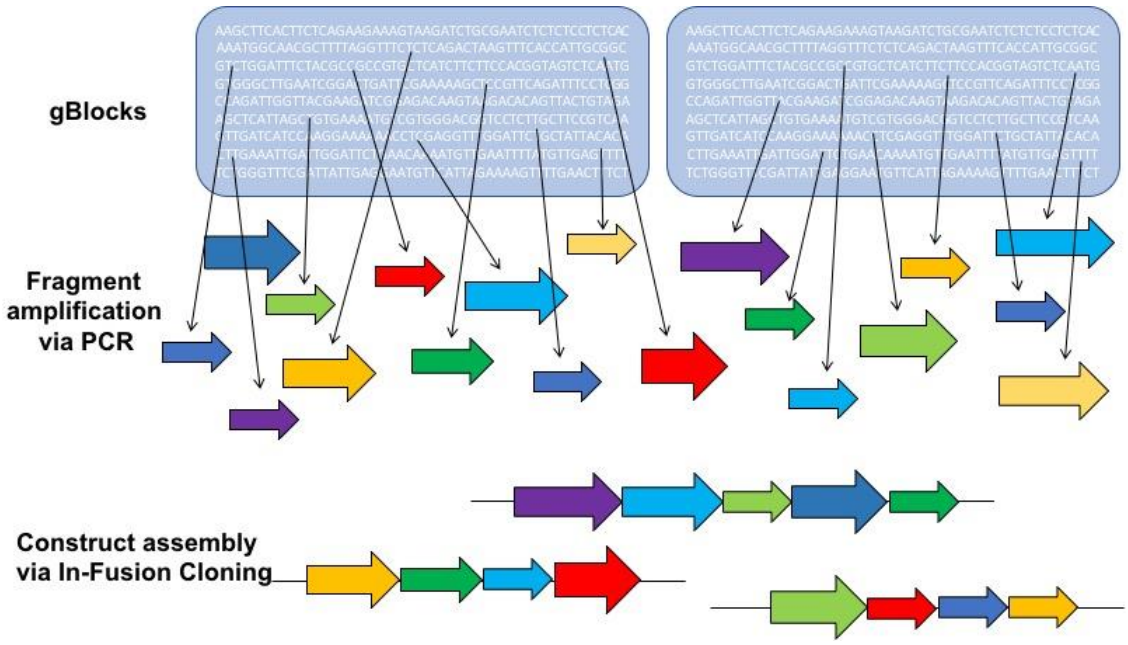

Figure 6. Workflow from gBlocks template to cloned constructs. gBlocks were cloned and used at a template for PCR. Fragments amplified with specific primers were then cloned into expression vectors via in-fusion multiple fragment cloning, which can assemble up to 5 fragments in a single reaction.

Preliminary testing of Constructs in *Nicotiana benthamiana*

Preliminary testing of Split GFP constructs

In typical experiments involving assembly of separate GFP fragments, the GFP coding sequence is split between the 6th and 7th beta sheets. Due to concerns about interfering with ribosome function or interactions if a too large a protein was linked to ribosomal protein 18B (RPL18B AT3G05590, RPL thereafter), smaller fragments of GFP were desirable. We tested refolding of two different GFP splits: Fragments consisting of beta sheets 1 through 9 (hereafter called GFP1-9) were tested for refolding with the corresponding fragment consisting of beta sheets 10 and 11 (GFP10-11). A second set was tested, consisting of beta sheets 1 through 10 (GFP1-10), with the corresponding 11th beta sheet (GFP11). The GFP1-9 and GFP1-10 constructs contained the flag purification tag at the N-terminus, to facilitate accessibility of the tag to the beads for immunoprecipitation. In addition, we compared the position of the cMyc tag located on the construct containing RPL: cMyc was positioned either in N-terminus of the protein (i.e., at the N-terminus of the GFP fragment), or between the GFP fragment and the N-terminus of the RPL coding region (Figure 7). As controls, we made constructs for flag-GFP-cMyc-RPL as well as flag-GFP.

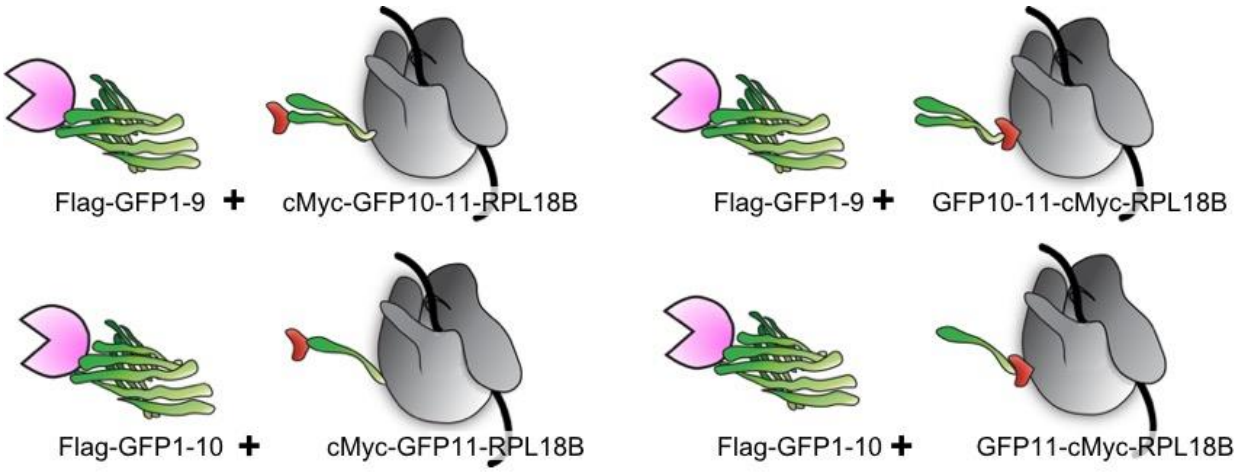

Figure 7. Diagrams representing the constructs tested for use in a split fusion-protein driven method to attach a purification tag to an endogenous ribosome. In these experiments, different splits of GFP and different positions of a constitutive cMyc tag were tested.

Preliminary testing and comparison of Split GFP-RPL constructs

Constructs containing different splits of GFP as well as different positions of spacers and tags associated with RPL were used to transform agrobacterium for transient expression in *Nicotiana benthamiana*. This method allows for our proteins of interest to be transiently expressed in plant cells in a matter of days, via infiltration of the transformed agrobacterium to the plant leaves and transient transformation of plant cells with T-DNA containing the genes of interest [52]. This was done to determine if addition or position of purification tags would interfere with ribosome function/localization, or GFP re-folding and/or fluorescence. These aspects were assessed with confocal microscopy to visualize GFP activity and Western blotting combined with immunoprecipitation, as described below.

We first compared the two splits of GFP. *N. benthamiana* leaves were imaged via confocal microscopy at various times, from as early as 2 dpi (days post infection) and as late as 14 dpi following agro-infiltration. Fluorescence was first seen at 2 dpi and further experiments focused on 3, 5, and 7 dpi time points. These time points were selected based on the downstream needs for the system to be applied to interactions with *Hpa*, for which the lifecycle is typically completed in 7 days under the conditions in our lab.

We observed that the two different splits of the GFP did not show the same intensity of fluorescence when expressed with RPL18 (figure 8). Fluorescence from the GFP1-9/GFP10-11 split was noticeably brighter than from the GFP1-10/GFP11 split at all time points. Additionally, the position of the cMyc tag affected the intensity of GFP fluorescence. Interestingly, the GFP1-9/GFP10-11-cMyc-RPL showed slightly brighter fluorescence, with a localization more similar to that observed for the free GFP and GFP-cMyc-RPL samples. Additionally, we noted that there was very little fluorescence in the samples infiltrated with GFP1-10 + GFP11-cMyc-RPL. Agrobacterium was re-transformed with these clones and the infiltrations were repeated yielding the same results, leading us to believe that in this combination,

some aspect interferes either with GFP re-folding and fluorescence, or ribosome function or interactions.

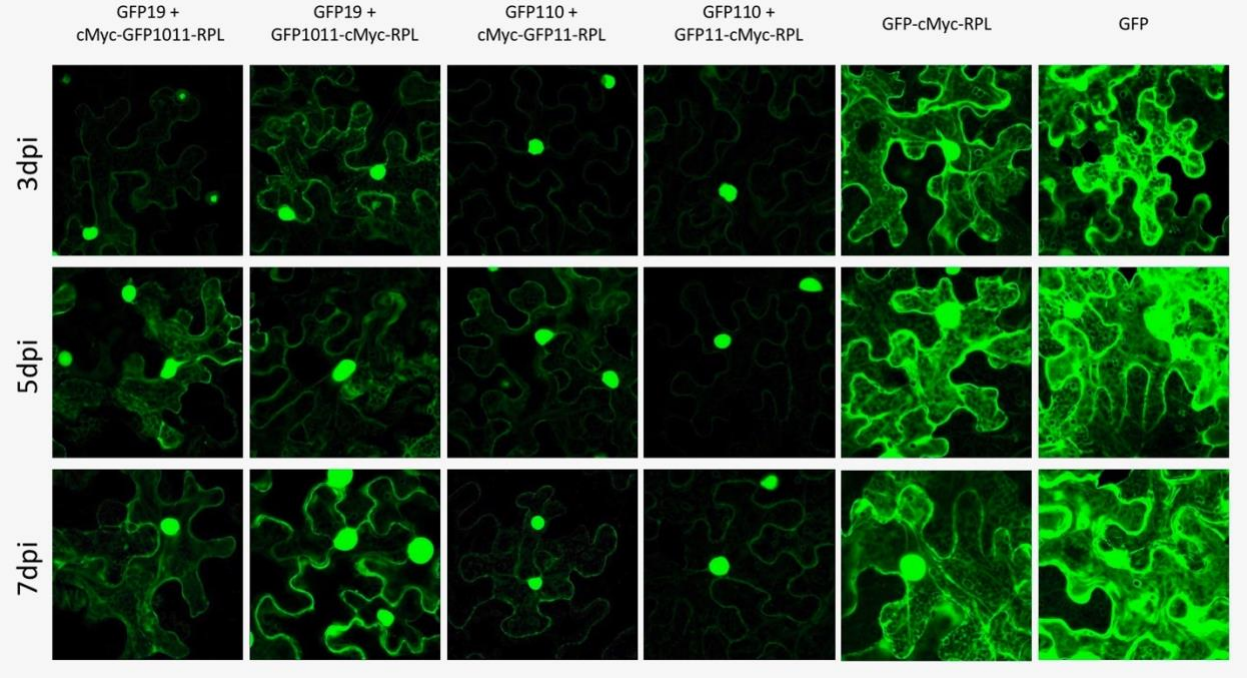

Figure 8. Comparison of GFP re-folding and fluorescence based on protein split and constitutive tag position. The GFP19 split shows more fluorescence than GFP110. Additionally, the position of the cMyc tag has an effect on fluorescence, although this affect varies according to the split of the GFP protein. Full GFP attached to the ribosomes and free GFP serve as controls.

To confirm that fluorescence correlates with an association of the flag purification tag to the ribosome, infiltrated tissue samples were harvested at 3, 5, and 7 dpi for western blotting experiments. Samples from 3 biological and technical replicates were pooled according to time point, and the tissue was used for a modified TRAP extraction (figure 9). To be certain that flag-GFP forms a strong association with the ribosome, and to test whether flag-GFP not associated to a ribosome would outcompete ribosomally-associated flag-GFP on the flag beads, a sucrose cushion step for isolation of polysomes was added to the TRAP protocol.

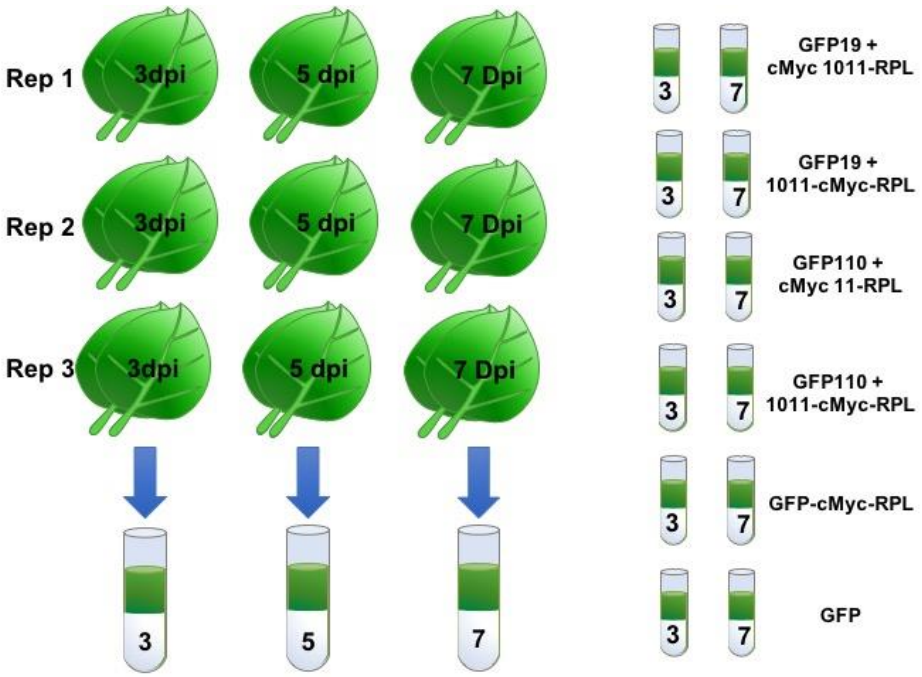

Figure 9. Experimental outline for polysome expression and extraction and purification. *N. benthamiana* leaves were infiltrated, tissues were harvested at 3, 5, and 7 dpi. Three biological replicated were performed and pooled for total combined analysis. Although tissue samples were collected at 5 dpi, only the 3 and 7 dpi timepoints were used for TRAP experiments.

While it was assumed that isolation via sucrose gradient would yield a polysome pellet from which concentrated amounts of ribosomes/polysomes could be purified, gel analysis of RNA extracted from early samples immunopurified from the pellets showed that there was little difference between RNA profile of clarified leaf extract (CLE) and immunopurified polysomes. In these samples, the two largest bands (25S and 18S) correspond to the large and small cytosolic ribosomal subunits. The four smaller bands correspond to chloroplastic and mitochondrial ribosomal subunits. In pure polysomal RNA samples from TRAP, we would expect to see an enrichment of the two largest bands, and very faint or no signal corresponding to the smaller bands from chloroplastic and mitochondrial ribosomal RNA subunits, because the chloroplastic and mitochondrial ribosomal subunits should be excluded by the gradient. Thus, further modification of the sucrose-cushion extraction method was required. To reduce potential aggregation of proteins to polysomes, the detergents used in the extraction buffer used to make the clarified leaf extract were added to the sucrose cushion. In addition, instead of using the recommended detergent-free resuspension buffer (via gentle pipetting after a 30 minute incubation), polysome pellets were resuspended overnight on a spinning wheel at 4°C in a larger volume of extraction buffer. This modified protocol is pictured in Figure 10. RNA extracted from the flag bead purification from these polysomes yielded an enrichment of ribosomal subunits when analyzed via RNA gel (Figure 10).

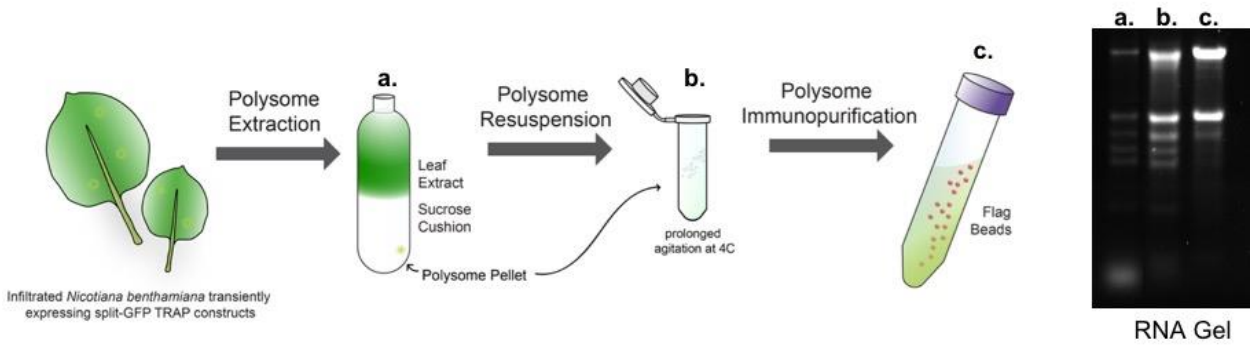

Figure 10. Polysome expression, extraction, resuspension, and purification. *N.benthamiana* leaves are infiltrated, the tissues were harvested and used for polysome extraction via differential centrifugation of CLE (a.) through a sucrose cushion. Polysomes are resuspended in a detergent buffer overnight (b.) and added to a flag bead solution for immunopurification (c.). RNA extracted from each step shows total RNA from CLE, RNA enriched with large and small ribosomal subunits from resuspended polysomes, and purified polysomal RNA from flag beads.

Samples corresponding to clarified leaf extract, polysomes (as found in the pellet present after centrifugation of the CLE over a sucrose cushion), and immunopurified polysomes associated with flag beads (immunopurified polysomes), were taken at three and seven dai. The protein content of each timepoint sample was examined via western blotting to assess the presence and accumulation of proteins from the various tested transgenes. In addition, RNA was extracted from these samples to determine if intact ribosomal RNA was present after immunopurification. We expected that the CLE should contain all expressed proteins, the polysome pellets should contain all proteins that are associated with ribosomes as well as free polysomes, and the final immunopurified polysome sample should be enriched with polysomes and ribosomes associated with a purification tag. We did not expect to see free GFP in the pellet or immunopurified polysomes samples, as it is not dense enough to penetrate the sucrose cushion.

Western blot analysis was performed with antibodies corresponding to flag (for the flag-GFP1-9 or flag-GFP1-10 fragments) or cMyc (for the GFP10-11-RPL or GFP11-RPL fragments) (figure 11). Expected band sizes are outlined in table 1. As expected, GFP is only detectable in pellet and enriched polysomes samples when fused to a protein that associates with a ribosome. The full-length GFP control samples, as well as the single-infiltration GFP1-9 and 1-10 samples, show no accumulation of GFP in pellet or immunopurified polysomes samples (pellet blots), but heavy accumulation is present in CLE at both time points (CLE blots). It is noted that no bands are present in GFP1-9 + cMyc-GFP10-11-RPL samples for α-flag treated CLE blots. Although fluorescence was present in these samples, and the flag-GFP is detectable in flag-bead samples, we could not detect a band from this time point even after several repeated blots. We do not know why this is the case.

For blots from the polysome pellet, only the GFP-RPL control is readily detectable with α-flag. This may be due to interactions with the detergent buffer and the flag tag in these samples. In an attempt to work around this issue, proteins were precipitated and resuspended in sample buffer. However, even then we were unable to detect flag-tagged proteins. However, since flag-tagged proteins

are readily detectable from immunoprecipitated samples it can be inferred that the proteins are present in the polysome pellet (as that is what flag beads are incubated with for immunopurification).

Table 1. Relative expected sizes of split GFP constructs

Containing	kDa for α-Flag	kDa for α-cMyc
GFP1-9 + cMyc-GFP10-11-RPL	23	29
GFP1-9 + GFP10-11-cMyc-RPL	23	29
GFP1-10 + cMyc-GFP11-RPL	26	26
GFP1-10 + GFP11-cMyc-RPL	26	26
GFP-cMyc-RPL	52	52
GFP	28	none

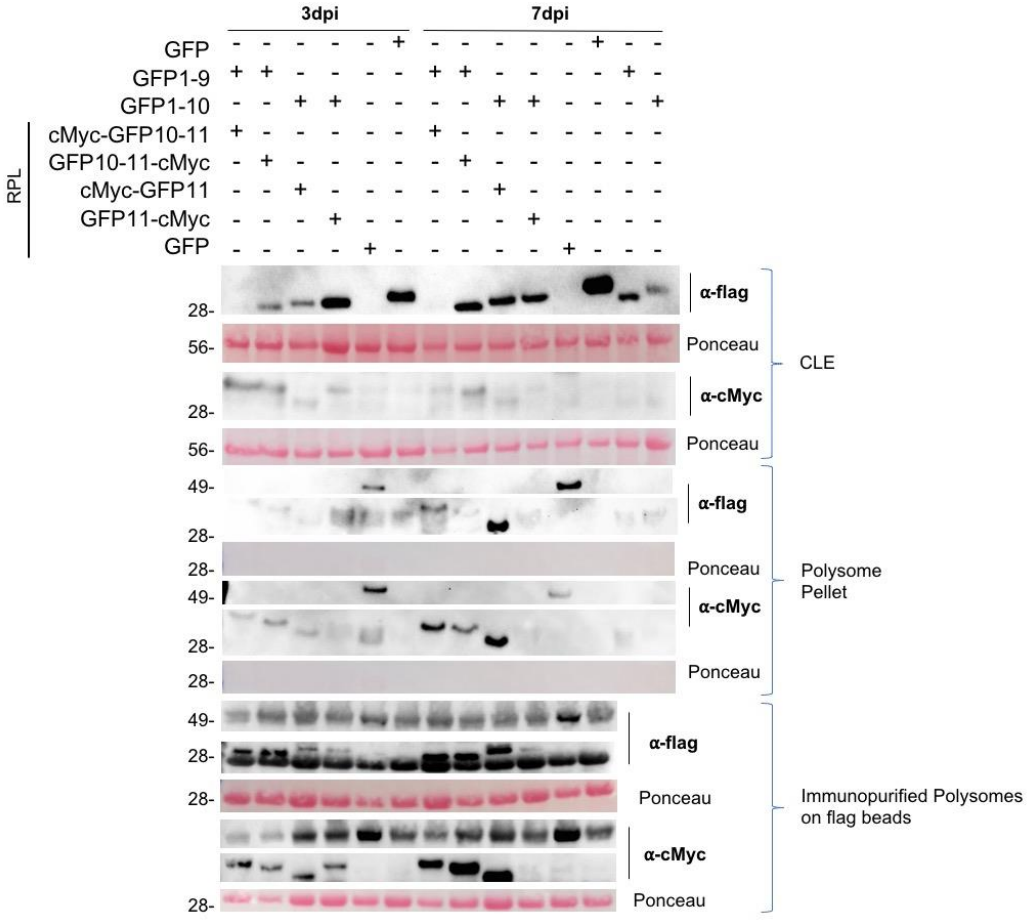

Figure 11. Western Blot of 3 and 7 dpi timepoints with samples from CLE, the polysome pellet, and immunopurified polysomes on flag beads. CLE samples containing all proteins were assayed with α-flag and α-cMyc to show accumulation of GFP1-9 or 1-10 fragments (α-flag) or GFP10-11-RPL or GFP110-RPL fragments (α-cMyc). GFP and RPL fragments should all be present in all samples. Polysomes pellet samples containing all proteins dense enough to penetrate the sucrose cushion were assayed with α-flag and α-cMyc to show accumulation of GFP1-9 or 1-10 fragments (α-flag) or GFP10-11-RPL or GFP110-RPL

fragments (α-cMyc). GFP fragments should only be present if associated with a ribosome at the time of extraction. Full GFP, GFP1-9 and GFP1-10 samples serve as negative controls. Flag beads with associated immunopurified proteins were assayed with α-flag and α-cMyc to show accumulation of GFP1-9 or 1-10 fragments (α-flag) or GFP10-11-RPL or GFP110-RPL fragments (α-cMyc). Flag beads, as they contain α-flag, conjugate with α-mouse and are therefore exposed as heavy (~50kda) and light (~25kDa) chains.

As noted in the fluorescence imaging, less flag-GFP was present in immunopurified samples for GFP1-10 + GFP10-11-cMyc-RPL at all experimental timepoints, indicating a lesser amount of refolding and association with ribosomes. The flag-GFP1-9-containing constructs and their associated GFP10-11-RPL counterparts were abundant in immunoprecipitated samples, indicating that a significant amount of re-folding/association occurred in these samples.

RNA was extracted from polysome pellets and immunopurified polysome samples for analysis via agarose gel electrophoresis and the Agilent 2100 bioanalyzer. Samples from the free GFP control were excluded from this analysis, since there was no GFP present in polysome pellets or immunopurified samples as shown on western blots, and RNA extraction from flag beads yielded no RNA, as expected. mRNA samples from immunoprecipitated GFP1-10-containing constructs had normal or very low yields, depending on the position of the cMyc tag, and this is apparent on the RNA gel as samples from GFP1-10 + GFP10-11-cMyc-RPL where the bands are very faint or not visible at all. This result is consistent with the low fluorescence seen during imaging as well as with the reduced abundance of tagged protein shown from western blotting. RNA gel analysis shows intact RNA extracted from resuspended polysome pellets at 3 and 7 dpi (figure 12). In the samples of RNA from immunopurified polysomes, the two bands from the large and small ribosomal subunits are enriched. This suggests that these samples contain a mostly immunopurified polysomes and ribosomes. We must note, however, that some mitochondrial and chloroplastic contamination is present. Together, these gel results indicate that the TRAP of polysomes from infiltrated *N.benthamiana* yields intact ribosomal RNA from polysomes that were tagged by the refolding of flag-GFP. Western blot, nanodrop quantification, and RNA gel analysis show that GFP1-9 samples, as well as the GFP-RPL control has the highest protein/RNA yields from immunopurification.

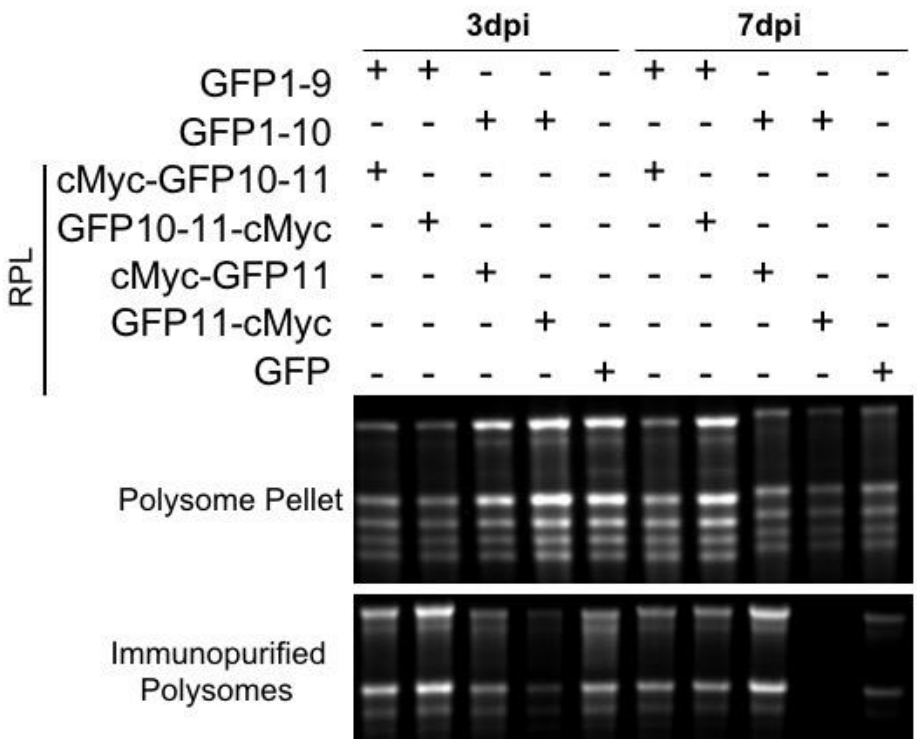

Figure 12. RNA gel analysis of polysome pellet and immunopurified polysome RNA samples from 3 and 7dpi. Split GFP and GFP-RPL control RNA samples from the polysome pellet or immunopurified polysomes at 3 and 7 dpi. Polysome pellet samples show all expected bands from large, small, chloroplastic, and mitochondrial origins. These samples were run with one µg of RNA. Immunopurified samples are enriched in large and small subunits, but bands from the chloroplast and mitochondria are still visible. These samples were run with total RNA extracted.

RNA from GFP1-9 samples as well as control GFP-RPL sample was analyzed via Agilent 2100 bioanalyzer to show that RNA from this method is of good enough quality for downstream applications such as sequencing. Bioanalyzer imaging shows in-tact total RNA present from polysome samples, as well as in-tact ribosomal RNA from immunopurified samples. The RNA Integrity Number (RIN) score is an algorithm that classifies RNA on a scale of 1-10, where 1 is most degraded and 10 is most intact [53]. RIN scores from all samples ranged from 7.9 to 8.7. These results indicated that when transiently expressed in *Nicotiana benthamiana*, split promoter-GFP constructs can be used to immunopurify polysomes, and the RNA extracted from the immunopurified protein is of high quality.

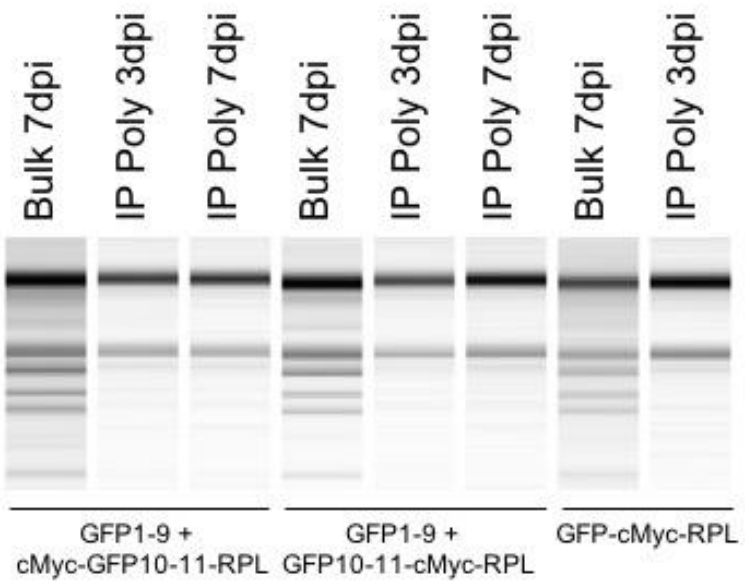

Figure 13. Bioanalyzer results. GFP1-9 samples as well as the GFP-RPL control were run with an Agilent 2100 Bioanalyzer. RNA Samples from polysome pellets (bulk) and immunopurified polysomes were loaded to show total RNA (as seen in Bulk) and ribosomes RNA (IP Poly samples). RNA as it is intact, and there is no distinguishable difference between GFP1-9 samples.

From the fluorescence microscopy assays, western blots, and RNA integrity test results, it was decided that GFP1-9 constructs performed better than GFP1-10 in refolding to their counterparts and securely attaching a purification tag to the ribosome. Regarding RNA amount and quality, there was very little discernable difference in performance between GFP1-9 + cMyc-GFP10-11-RPL and + GFP10-11-cMyc-RPL. The only concern that we had moving forward is that the cMyc tag between the GFP and RPL may promote cleavage of the flag-GFP from the ribosome. For these reasons, all further experiments were carried out with GFP1-9 + cMyc-GFP10-11-RPL construct.

To mimic an environment in which the flag-GFP fragment is induced and associated with an already-present GFP-RPL, dexamethasone-inducible constructs were created. Dexamethasone (Dex) is a synthetic corticosteroid that is not found in plants. It is used as a chemical induction agent in plants transformed with a chimeric transcription factor containing the receptor domain of the rat glucocorticoid receptor [54]. *N.benthamiana* was co-infiltrated with Dex-inducible flag-GFP constructs and GFP-RPL constructs. Fluorescence microscopy and western blotting confirmed that even without the application of dexamethasone, the “inducible” constructs were constitutively active. This may be due to the nature of the transient expression via agrobacterium. Therefore, these experiments were instead performed in stably transformed Arabidopsis, and discussed in chapter IV.

CHAPTER IV

Application of TRAP technology to plant-pathogen interactions

Moving the TRAP technology to Arabidopsis: The promoters

In order for the modified TRAP system to be used most efficiently in Arabidopsis, promoters must be chosen that allow for the desired cell specificity. Below are summaries of promoters that I evaluated for various goals of my project.

35S (CaMV35S) is a cauliflower mosaic viral promoter for transcription of entire genome. It has been well documented as a strong promoter with constitutive activity in almost every Arabidopsis cell type [55].

PETE2 (AT1G20340) is one of two Arabidopsis plastocyanin genes, involved in electron transfer in the chloroplast for photosynthesis. It is a negative regulator of translation, and functions in response to UV and copper ion homeostasis. The PETE2 promoter is active predominantly in mesophyll cells, where the majority of photosynthesis occurs [56] and where the majority of *Hpa* parasitism occurs.

RBCS2B (AT5G38420, Rubisco small subunit 2B) encodes a member of the Rubisco small subunit multigene family. RBCS2B has roles in carbon fixation, photorespiration, and responses to blue, far red, and red light. The RBCS2B promoter is active predominantly in the mesophyll [57].

PR1 (AT2G14610, Pathogenesis-related gene 1) is induced in response to a variety of pathogens and is used as a marker gene for SAR response, as it is salicylic-acid responsive. The PR1 promoter has been examined and used in several publications, and for our purposes we have selected the shortest effective promoter, which was 815bp [58]. The PR1 promoter was recently reported to be suppressed in Arabidopsis cells containing *Hpa* haustoria. Thus, I expected that the PR1 promoter would be active in cells that are proximal to but NOT in direct contact with those containing haustoria.

DMR6 (ATG5G24530, Downy Mildew Resistant 6) encodes a defense-associated gene that is required for susceptibility to *Hpa*. The promoter is active almost exclusively in cells that are in direct contact with pathogen haustoria [45].

DLO1 (AT4G10500, DMR6-Like Oxygenase 1) encodes a DMR6-like gene. The promoter has been described as active in vascular tissues near pathogen infection sites [59].

Attempts were made to transiently express these promoters in *Nicotiana benthamiana*. The transient expression was attempted in order test their cell-type specificity and efficiency and induction in the presence of an oomycete pathogen (*Phytophthora capsici*). These tests were carried out by infecting leaves with plugs containing transgenic *P. capsici* expressing mCherry under the Ham34 promoter [60]. Infected leaves could then be analyzed for fluorescence in which leaf cells would fluoresce green from the GFP re-folding, and the pathogen growth could be visualized in red. Results were encouraging at first. However, due to the nature of *Nicotiana benthamiana* or the efficiency of transformation by agrobacterium, the promoters expressed GFP constitutively without regards to

tissue/pathogen presence. In the case of PR1, expression was suppressed by the agrobacterium (as a pathogen itself) and little to no fluorescence was detected.

To directly test the activity of promoters in Arabidopsis, fusions to the GUS reporter gene were made for all of the chosen promoters. Constructs were introduced into Arabidopsis, and single-insertion homozygous lines were tested for promoter expression prior to and during infection with *Hpa*. DMR6 promoter-GUS expression was evident in increasing amounts from 3 dpi onward from seedlings that were inoculated 11 days after germination. However, GUS staining seemed to be more broadly localized then we would expect to see if it were associated solely with haustoria (and therefore would have followed a hyphal pattern of staining) (figure 14).

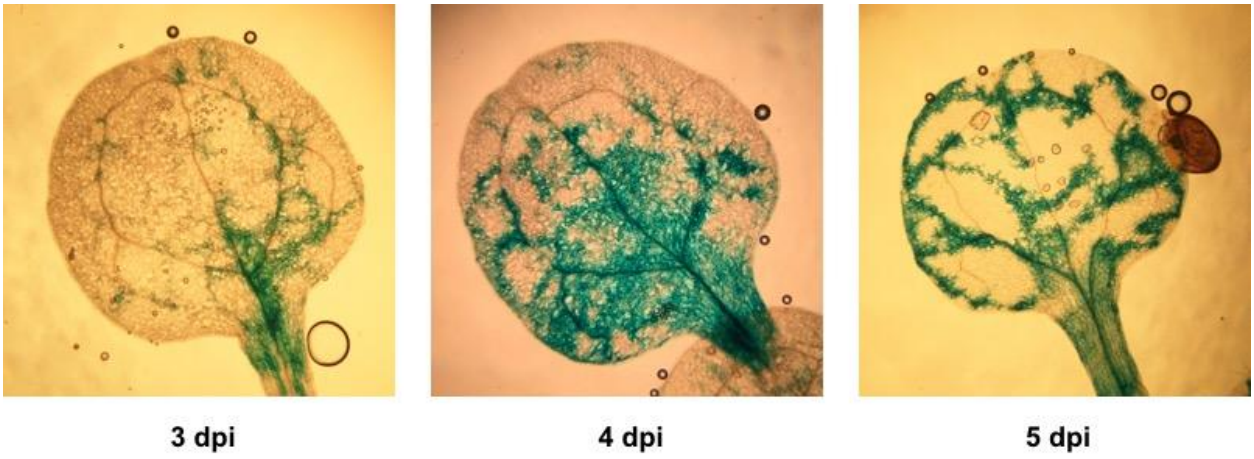

Figure 14. DMR6pro:GUS staining from 3-5dpi on infected Arabidopsis cotyledons. Staining is present in small amounts at 3dpi and shows an increase of promoter activity as the infection by *Hpa* progresses.

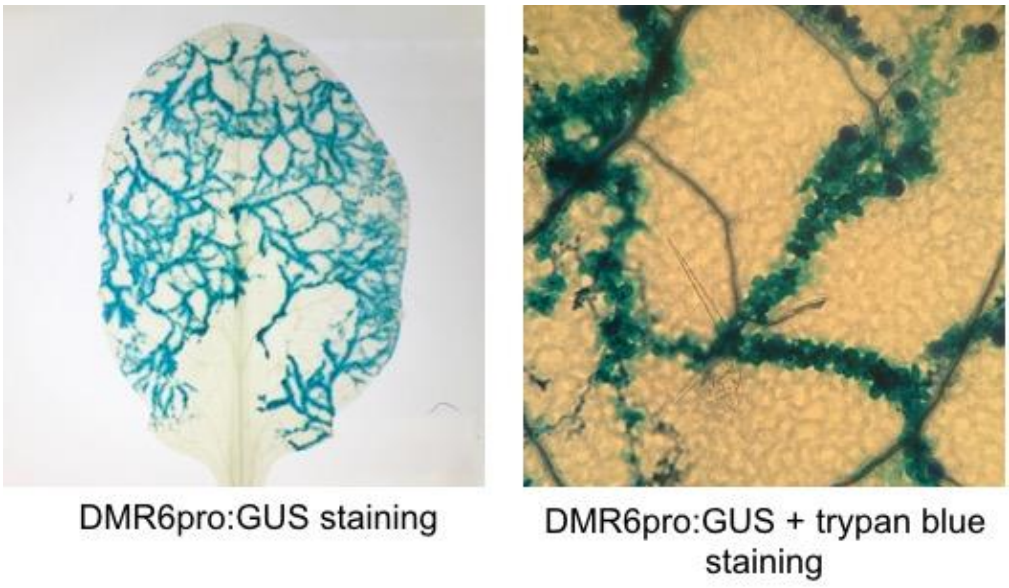

Figure 15. DMR6pro:GUS and trypan staining at 6dpi on infected Arabidopsis leaves. DMR6pro:GUS staining of infected leaves at 6dpi. Plants are 3 weeks old. Staining and is localized to haustoriated cells, stained by trypan blue.

Contastingly, DMR6 promoter-GUS activity was more tightly localized in true leaves of plants inoculated at 3 weeks after germination. GUS activity followed a hyphal pattern, and when co-stained with trypan blue it was evident that GUS activity was present predominantly in haustoriated cells (Figure 14, 15).

In the case of our mesophyll-specific promoters, PETE2-GUS showed even staining of mesophyll tissue with an absence of staining in all major veins (Fig 16).

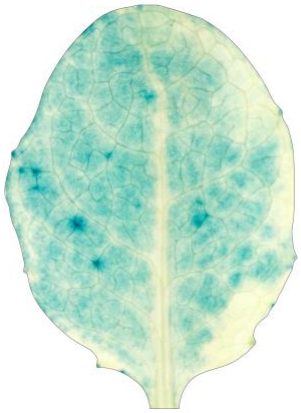

Figure 16. PETEpro:GUS staining of 3 week old Arabidopsis leaf. PETEpro:GUS activity showing localization primarily in mesophyll tissue. No activity is present in major veins/ vascular tissue.

PR1 promoter-GUS expression was difficult to interpret based on our experiments. According to qPCR analysis, PR1 expression can be expected to peak at 3 dpi and drop off as the infection progresses [10]. In addition, publications have shown GUS activity that is excluded from haustoriated cells and present in neighboring cells. Our PR1-GUS plants showed mixed results. GUS staining was only present from 4 dpi onward, and there was no PR1-GUS activity visible in cotyledons at any point during infection. (figure 17). In three-week old true leaves, PR-1-GUS activity would sometimes present as described in the literature (excluded from haustoriated cells) and other times not at all (staining in and around haustoriated cells) (figure 18). No staining was present in any DLO1 samples.

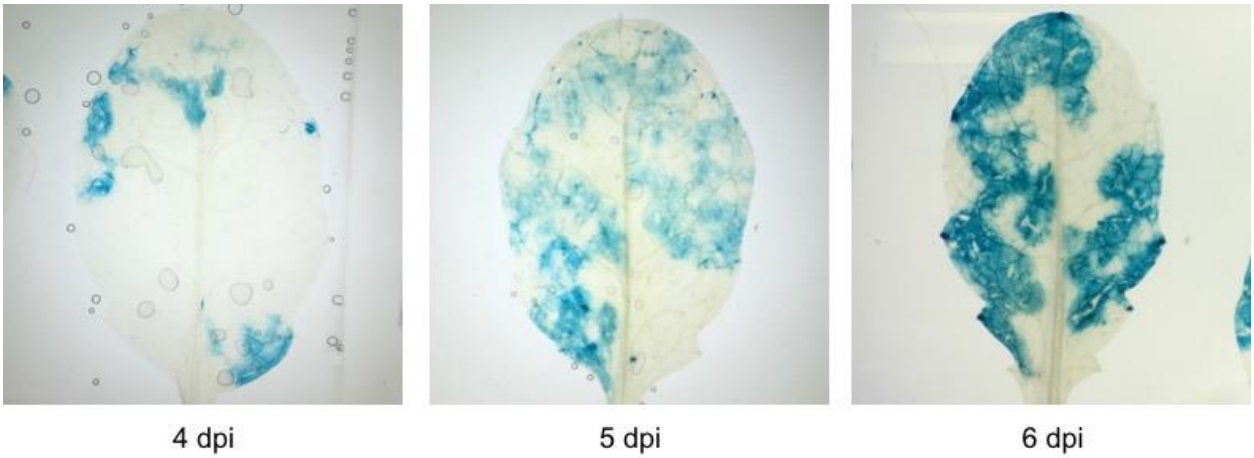

Figure 17. PR1pro:GUS staining from 4-6dpi on *Hpa*-infected Arabidopsis. PR1pro:GUS staining of infected four-week old leaves at 4-6dpi. Staining shows an increase of promoter activity as the infect progresses.

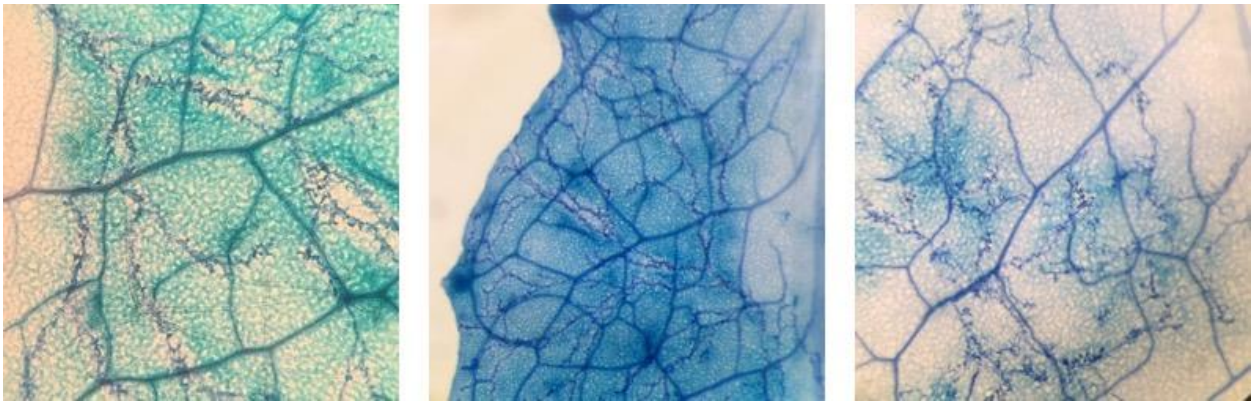

Figure 18. PR1pro:GUS and trypan co-staining of infected leaves. PR1pro:GUS and trypan staining of infected three-week old leaves at 6dpi. GUS staining shows variable localization. In some cases, staining is excluded from haustoriated cells. In other samples, staining is not excluded from haustoriated cells.

From these GUS results we were confident in our ability to replicate the results previously shown for DMR6 activity and localization under in-house conditions. Therefore, we were confident in the use of the DMR6 promoter in our TRAP system. As for PR1 and DLO1, our results did not match published results, and we were therefore less confident about their utility in the TRAP system. Although we introduced all promoter-TRAP constructs into Arabidopsis via floral dip and collected seed for all constructs, we subsequently focused on lines that contained the DMR6 and PETE promoters.

Testing DEX-inducible split GFP re-folding and association with the ribosome

To further analyze the activity of split GFP-RPL constructs under inducible vs constitutive conditions in Arabidopsis, a dexamethasone-inducible construct was made to control induction of Flag-GFP1-9. This construct allows for the induction of both the GFP1-9, and GUS as a secondary confirmation of activation. Arabidopsis plants were co-transformed with dexamethasone-inducible flag-GFP1-9 as well as constitutively active PETE-cMyc-GFP10-11-RPL via floral dip with Agrobacterium. Primary transformants containing both transgenes were selected and were assayed in the T1 generation for "leaky" expression via GUS staining prior to dexamethasone application, as well as induction via GUS

staining at 24hrs post dexamethasone application. X lines were selected to carry forward for further analysis in the T2 generation.

T2 plants were tested for segregation, and lines that had ratios near 3:1 to indicate a single insertion locus for each construct were used for preliminary induction experiments. 2.5-week-old seedlings were treated with 50 µM dexamethasone and assayed for GUS activity as well as GFP fluorescence. GUS staining was performed at 24 h post-dexamethasone application and showed somewhat even staining of leaves (figure 19). Leaves were assayed for fluorescence via confocal microscopy at 72 hours and four days post- application. No fluorescence was detectable at either time point, indicating as potential issue with expression and/or folding of the GFP. In order to troubleshoot the lack of fluorescence, CLE was assayed via western blot to confirm the presence of cMyc-GFP10-11-RPL. From this, cMyc-GFP10-11-RPL was detectable, indicating that more troubleshooting is needed to understand the lack of fluorescence.

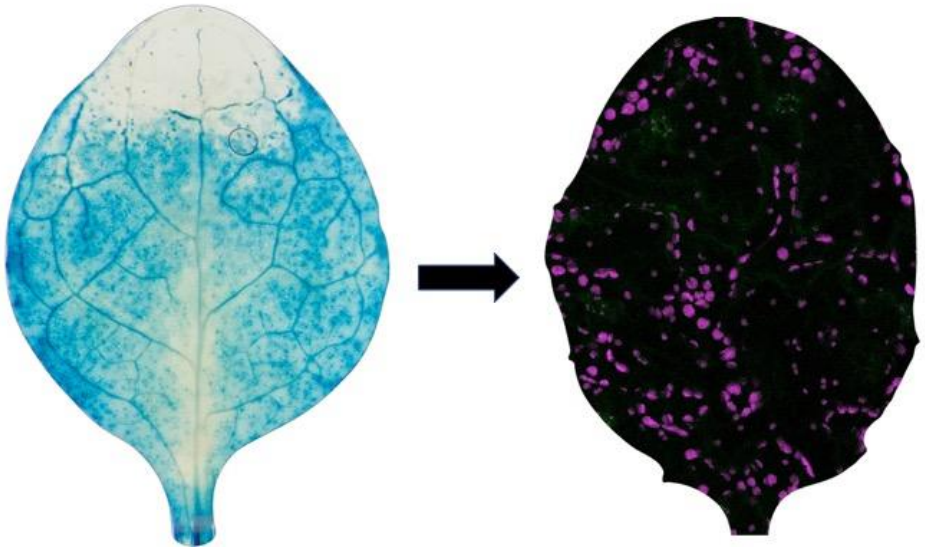

Figure 19. GUS staining and Fluorescence present after dexamethasone application. GUS staining indicating activation of the downstream components of the dexamethasone-inducible construct (left) does not translate into fluorescence, as shown by the leaf-shaped depiction of chlorophyll autofluorescence and barely-distinguishable GFP fluorescence (right).

Transformation of Arabidopsis with Promoter-TRAP constructs

Although attempts were made to narrow down and select candidate vectors based on transient expression in Nicotiana and promoter GUS activity, it was decided that several promoter combinations would be used to stably Arabidopsis and screened further in their intended experimental system. These lines are outline in table 2. All lines contain the inducible promoter-flag-GFP1-9 split and the constitutive promoter-cMyc-GFP10-11-RPL constructs. These gene fusions were transferred from the expression vectors for *Nicotiana* infiltration into an Arabidopsis transformation vector. The Arabidopsis transformation vectors carried two gene fusions each, one with the inducible promoter and one with the constitutive promoter, separated by a matrix-attachment region (figure 20). This matrix-attachment

region (TBS V26- a transformation booster sequence from petunia) allows for expression of both promoters without compromising the function of either [61]. All lines were transformed via floral dip into Col0 and carried kanamycin resistance for selection and segregation counting.

Table 2. Outline of Promoter-TRAP constructs for transformation of Arabidopsis

Line #	Clone #	Promoter-flag-GFP1-9	Promoter-cMyc-GFP10-11-RPL
412	774	DMR6	35S
413	775	DMR6	Rbcs2B
414	776	DMR6	PETE2
415	779	DLO1	PETE2
416	780	PR1	35S
417	782	PR1	PETE2
418	784	35S	Rbcs2B
419	785	35S	PETE2
420	777	DLO1	35S
421	781	PR1	Rbcs2B

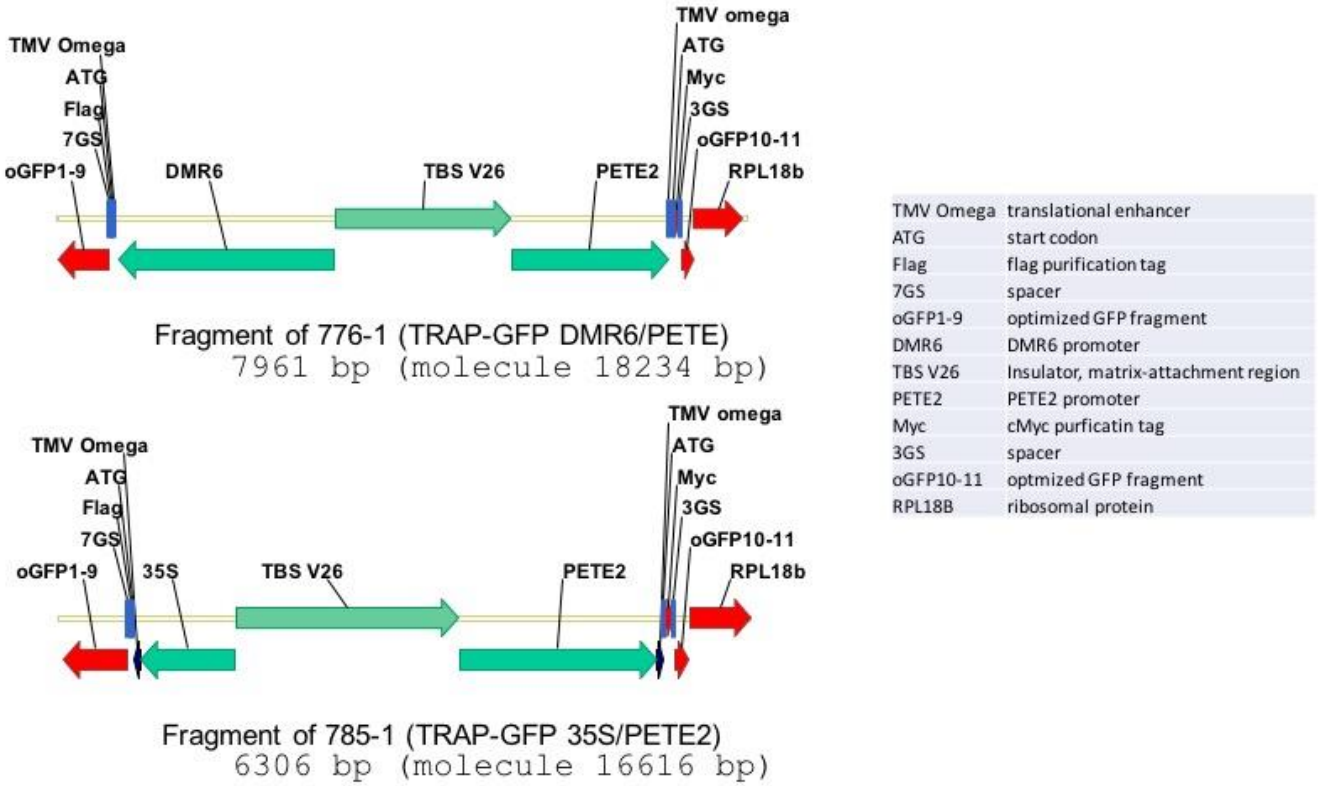

Figure 20. promoter-TRAP constructs. VectorNTI images of constructs used to create transgenic Arabidopsis for TRAP experiments. Each construct contains two promoter-driven components, separated by the TBS V26 insulator.

Final line selection and outline of the TRAP experiments

From the transformed Arabidopsis, representative lines were chosen based primarily on fluorescence phenotypes present when challenged with *Hpa*. Strong fluorescence was seen from several representative lines as shown in figure 21. The initial goal was to identify one line for each promoter set for experiments to gather RNA sequencing data. However, upon review of the resources allocated for the sequencing, depth of sequencing required for a robust data set, and the performance of the various promoters in our experimental conditions, it was decided that only two lines (414C4 and 419F2 corresponding to DMR6 and 35S- PETE combinations (figure 22)) would be used for the initial TRAP experiments for RNAseq. PR1 was de-prioritized due to low confidence in the reproducibility of its expression, as well as issues with the construct and visualization of fluorescence. DLO1 was discarded not only because of lack of expression, but in addition due to lack of a control cell set for data comparison. Importantly, by de-prioritizing these lines, we were also able to allocate our RNAseq budget to include additional samples that would allow for comparison of the *Hpa*-induced transcriptome and translatome on a whole-leaf level, as described below.

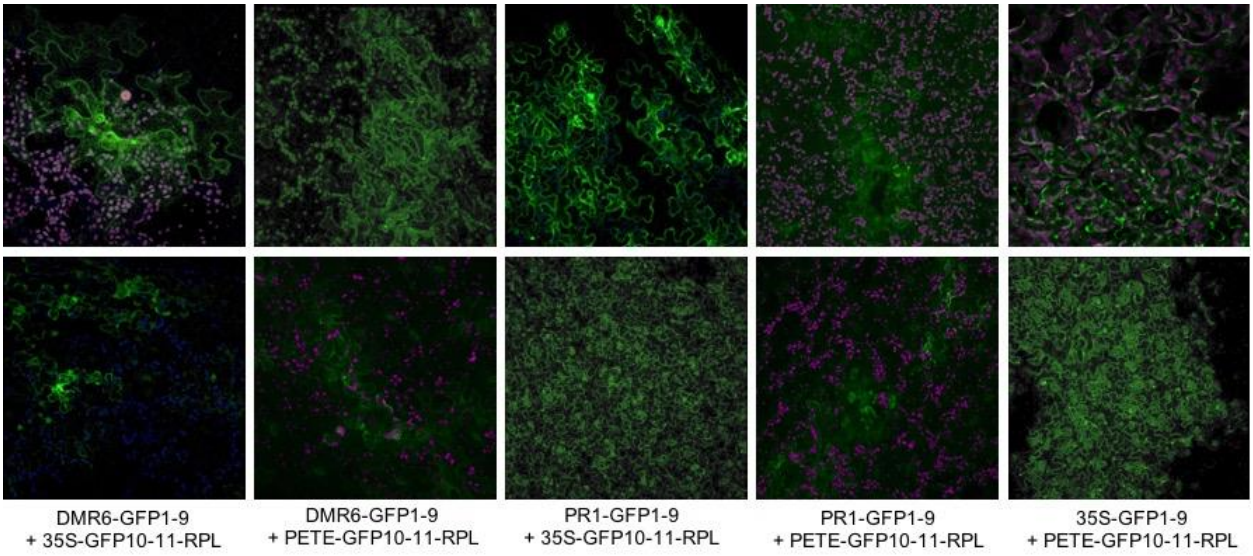

Figure 21. Confocal imaging of infected promoter-GFP/RPL lines at 6dpi. The DMR6 promoter drives expression of flag-GFP in combination with 35S-GFP-RPL or PETE-GFP-RPL respectively and these lines show fluorescence localized in haustoriated cells. The PR1 promoter driving expression of flag-GFP in combination with 35S-GFP-RPL or PETE-GFP-RPL respectively, and these lines show fluorescence localized in pathogen-distal cells. The line containing 35S-GFP and PETE-GFP-RPL constructs shows fluorescence heavily localized in mesophyll cells, regardless of pathogen activity.

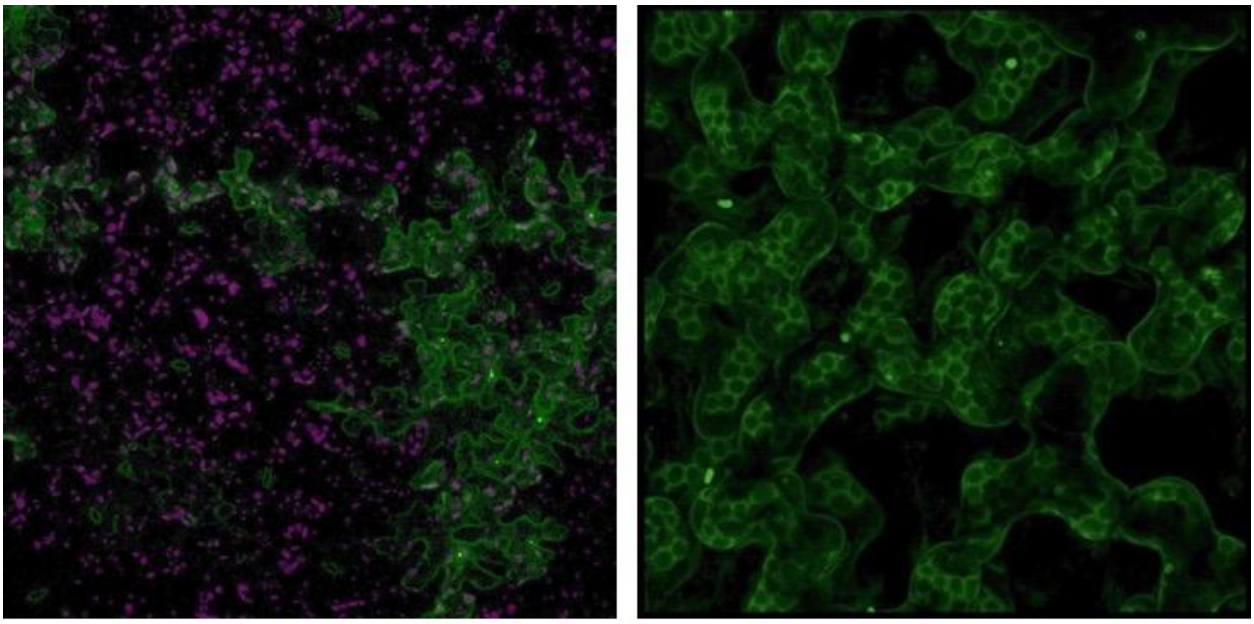

Figure 22. Confocal imaging candidate promoter-GFP/RPL. At 6dpi, infected DMR6-GFP1-9 + PETE-GFP10-11-RPL (line 414C4) shows fluorescence localized in haustoriated cells. Line 419F2 containing the 35S-GFP1-9 + PETE-GFP10-11-RPL constructs shows fluorescence heavily localized in mesophyll cells, regardless of pathogen activity.

In addition to determining the two lines to be used for RNA sequencing data collection, time points from the pathogen infection and the TRAP protocol itself needed to be determined. Based on the need for as much RNA as possible (and therefor as much tagged ribosomes as possible), the 6 dpi time point was chosen. This is the last day *Hpa* grows within the leaf before sporulation, and therefore it is the timepoint in which the most haustoriated cells are present during the life cycle. These samples were processed through the TRAP protocol and RNA was collected from the CLE for total RNA sequencing in addition to the IP RNA samples. Mock treated samples (sprayed with water instead of spore solution) were collected as well for total RNA samples from 414C4 (since no tagged ribosome would be present) and for total RNA and TRAP RNA from line 419F2.

These data will allow us to attempt to answer several questions. First, is there a significant difference between transcriptional and translational control? Does this difference change in the presence of a pathogen within the plant? How much of the change that we see is due to overall plant stress? These can be answered by comparisons of 419F2 translatome vs transcriptome for both uninfected and infected samples, as well as a comparison of the infected 419F2 translatome to the uninfected translatome.

Another equally important question to analyze is if there is a difference in gene expression within haustoriated cells as compared to other cells. Is there a difference between the translatome of haustoriated mesophyll cells as compared with the entire mesophyll's translatome (comprised of both haustoriated and non-haustoriated cells)? Is there a significant difference between the translatome of

haustoriated cells and the whole leaf transcriptome? How does the translatome of haustoriated cells compare to the translatome of non-infected mesophyll cells? To analyze these questions, we can compare the translatome of 414C4 with that of infected 419F2, the translatome of 414C4 with the infected total RNA from the same line, and the 414C4 translatome with the translatome of uninfected 419F2. In addition to questions about translatome vs. transcriptome and haustoriated vs. total cells, these data will allow us to take into consideration controls such as infected vs uninfected transcriptome. The full set of comparisons available from these lines at the 6 dpi timepoint are outlined in figure 23.

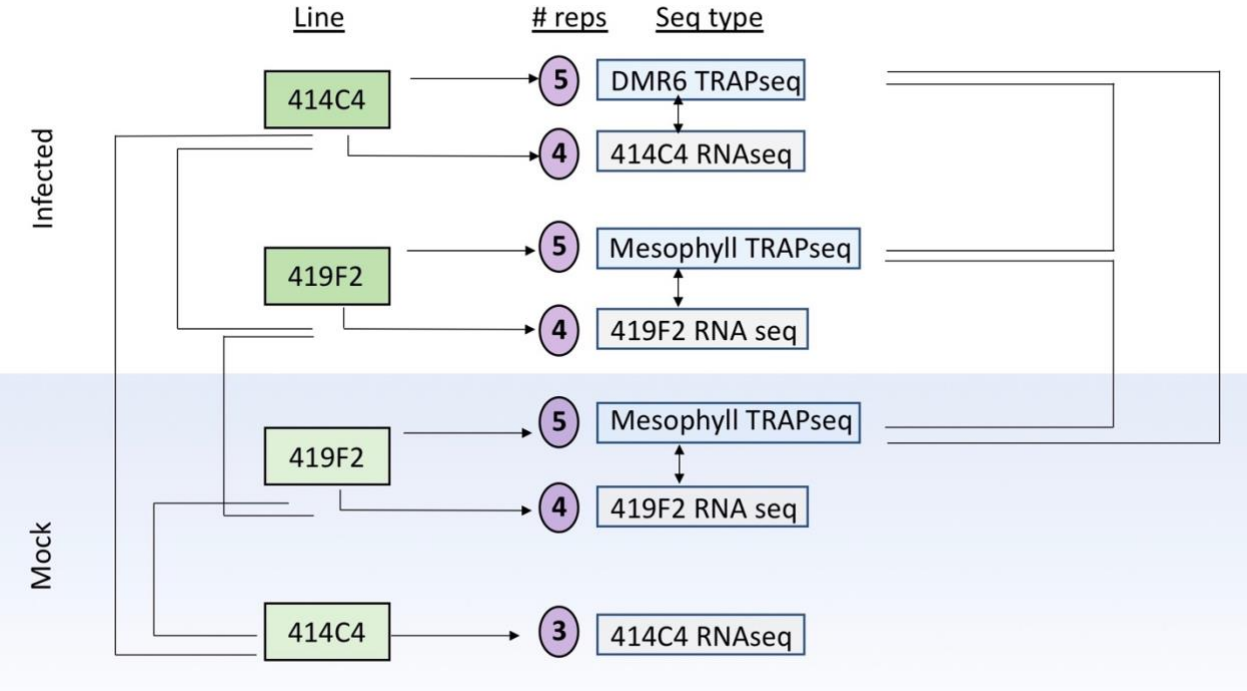

Figure 23. TRAP experimental comparisons. RNA from different conditions, lines, and timepoints in the TRAP extraction will be sequenced and used for multiple comparisons. These comparisons include infected vs. uninfected, total RNA sequencing vs. TRAP sequencing, and RNA (both total and TRAP) from haustoriated cells vs. from all cells. The number of biological replicates sent for sequencing varies from 3 to 5.

CHAPTER V

The TRAP experiments/ sample preparation for sequencing

Replicate selection

TRAP experiments were replicated 15 times, with bulk tissue collected at 6 dpi (either mock treated with water or infected with *Hpa*) from lines 414C4 and 419F2. In parallel, additional samples were collected for DNA extraction (to be used for qPCR to analyze relative pathogen load in the plant), trypan blue staining (for visualization of hyphal colonization), and for confocal microscopy (to visualize refolding of the GFP and hence fluorescence as well as the attachment of the purification tag to the ribosomes). Additionally, at 0, 4, and 6 dpi, samples were collected for RNA extraction and RT-qPCR to analyze marker gene expression over the course of infection. These data allowed us to select replicates

that carried an equal amount of pathogen load and had “normal” marker gene expression throughout the course of infection.

DNA samples were used for quantitative PCR to assess pathogen load in the leaves [62]. Pathogen load across all samples was fairly similar (figure 24a). Trypan blue stains from the same timepoint indicated normal hyphal growth and an equal relative amount of visible hyphae within the leaf (figure 24b). From these results, we selected replicates to evaluate further. RT-qPCR was performed with RNA from the 0, 4, and 6 dpi timepoints using markers genes for Actin2 (housekeeping gene), PR1 (for general plant stress), DMR6 (for pathogen response), GFP1-9 (to confirm promoter activity), PDF1.2 (for ABA) and COR15A (for JA) (figure 25). Together, these marker genes were used to confirm that plants were not in a state of stress prior to infection, and that the replicated responds in a similar fashion throughout their interactions with *Hpa*. In infected replicates, PR1 expression is expected to be very low at 0dpi, and higher as infection progresses. DMR6 expression is expected to follow a similar trend, with induction occurring with infection. In line 414C4 (in which GFP is under the control of the DMR6 promoter, expression is also pathogen-inducible although expression is low compared to other marker genes (figure 25 a, b). In non-infected replicates, there should be little to no PR1 or DMR6 activity. Line 414C4 shows no GFP activity, and line 419F2 (in which GFP is under the control of a constitutive promoter) shows normal, consistent expression of GFP (figure 25 c, d). In infected replicates, it was difficult to discern activity patterns PDF1.2 and COR15A. This may be due to the nature of the plant-pathogen interactions, and therefore these results were excluded from our decision process for replicate selection of infected samples. Confocal microscopy was also performed at 6dpi as a visual confirmation of association of Flag-GFP1-9 with ribosomal proteins in the appropriate cell types for each line.

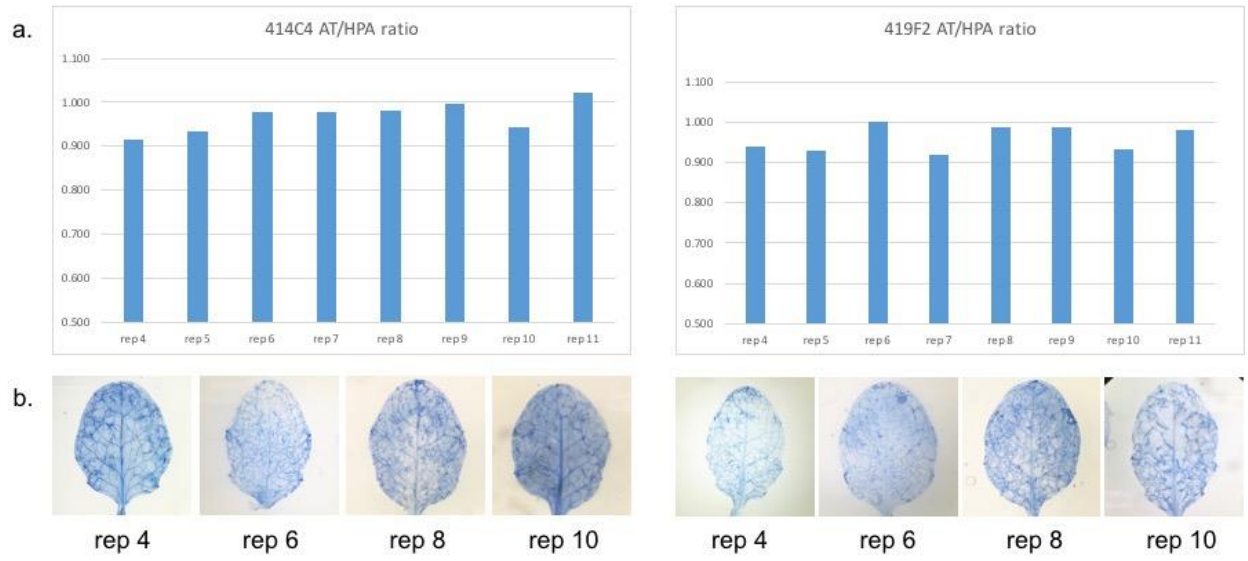

Figure 24. Pathogen load assays for replicate selection. For qPCR analysis, DNA was extracted from Arabidopsis leaves at 6 dpi and used for Taqman qPCR with primers/probes corresponding to Arabidopsis actin and *Hpa* actin (a.). Ratios were calculated from the cycle numbers for each actin primer set. Trypan blue staining was also performed at 6dpi for a visual representation of pathogen growth in the leaf (b.).

a. 414C4 (DMR6-GFP19 + PETE-GFP1011-RPL) INFECTED REPS

b. 419F2 (35S-GFP19 + PETE-GFP1011-RPL) INFECTED REPS

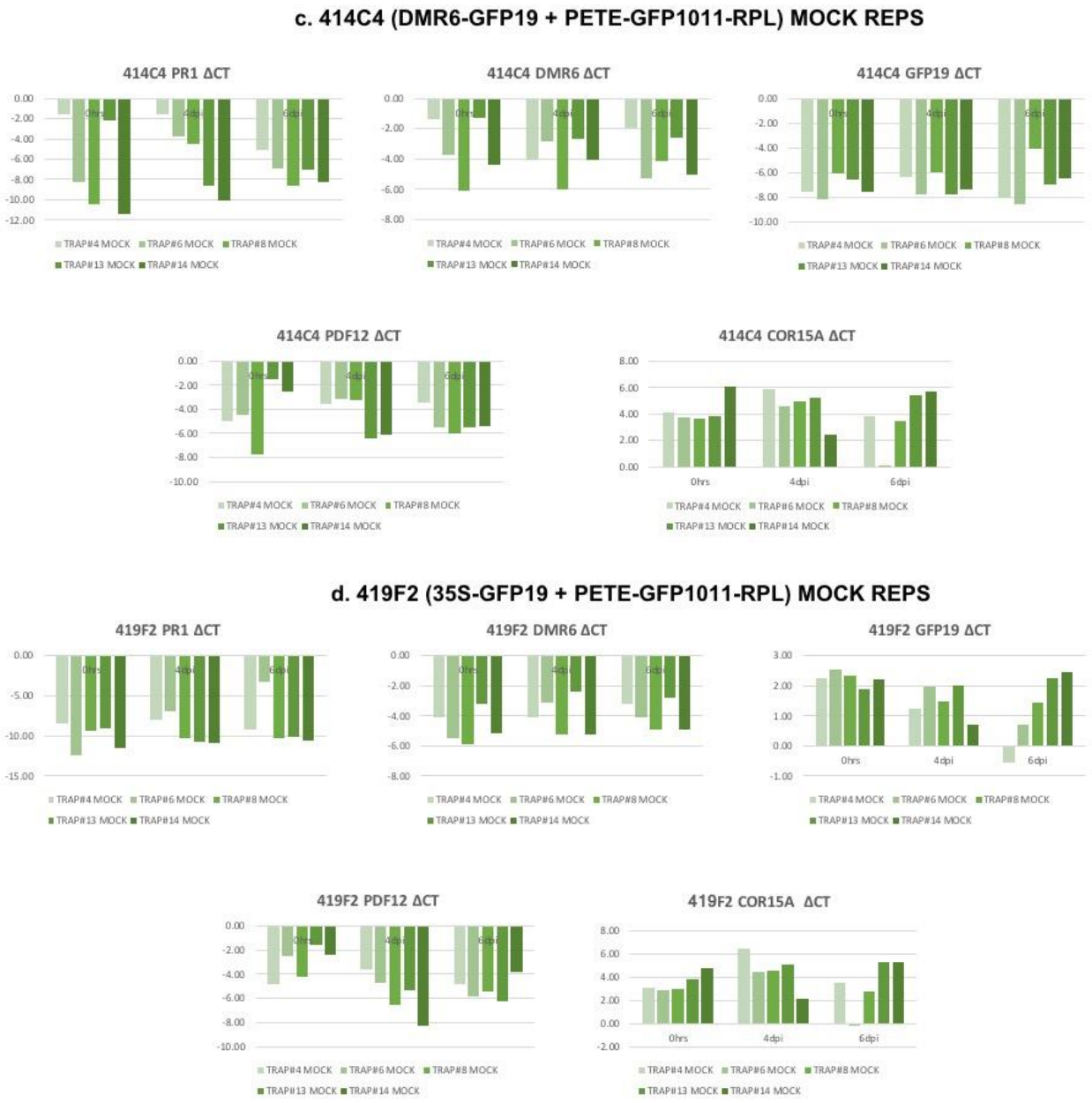

Figure 25. qPCR analysis of plant stress marker genes. Samples candidates for TRAP and RNA sequencing were analyzed by RT qPCR using the ΔCT method with housekeeping gene actin. Infected (a, b) and uninfected (c, d) samples showed expected expression patterns in most cases.

TRAP methods: The trade-off between amount of RNA and quality of the samples

When approaching the purification protocol for the Arabidopsis samples, a decision had to be made regarding the use of the sucrose cushion, based on the following trade-off: the sucrose-cushion method may yield a higher amount of RNA for sequencing, but based on RNA gel analysis, it may not contain only polysomes/ ribosomal proteins and therefore have some RNA contamination. To address this concern, a comparison was made between the RNA gathered from direct purification from CLE to

beads (“direct” purification) versus the RNA gathered from first pelleting the polysomes through the sucrose cushion and then using bead purification (“cushion” purification).

RT-qPCR was performed using marker genes for Actin, 18S, 25S, RBCS, RBCL, SUC2a, and *Hpa* Actin (figure 26). Although not large, there was a difference between the two purification methods as it regards RNA content. It was interesting to note that *HPA* Actin was slightly enriched in both methods, although more in the cushion sample. In addition, SUC2a was amplified in a similar manner. Both of these marker genes were intended to be negative controls, and the fact that enrichment was present for both bring to light the understanding that although ribosomes and polysomes are immunopurified prior to RNA extraction, contamination will occur. It also brought to light that although tagged ribosomes are coming from mesophyll cells, some contamination from other cell types, such as vascular tissue, can occur. From this, it was decided that the direct purification method would yield the more pure RNA sample and therefor was a more accurate choice for RNA sequencing.

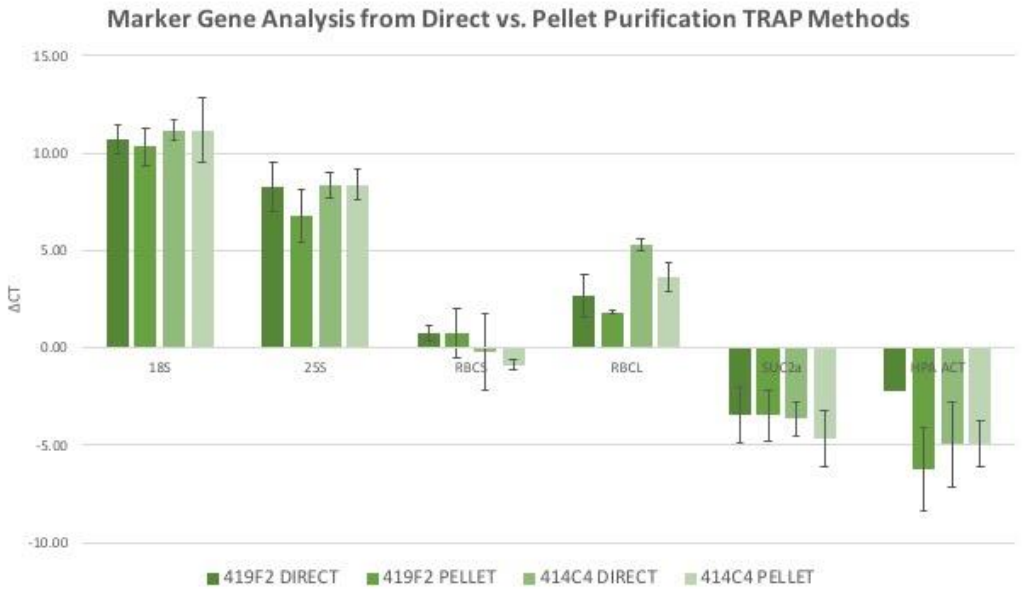

Figure 26. qPCR analysis marker gene expression in samples from direct and pelleted TRAP experiments. RT qPCR was performed to quantify expression of several plant marker genes in samples from immunopurified polysomes. Polysomes were immunopurified by the direct or pelleted methods. Values are displayed as delta Ct, where the Ct value of the gene of interest was subtracted from the Ct value of the housekeeping gene, Actin. Negative values indicate lower gene expression, positive values indicate higher gene expression.

Polysome Immunopurification and RNA integrity

Immunopurification was performed from CLE from all samples except the mock-treated 414C4 sample, from which only total RNA was collected. RNA was quantitated, and it is of interest to note that uninfected samples yielded about 40% more RNA than infected samples (in the case of line 419F2) (table 3), further supporting the hypothesis that ribosome biogenesis or stability may be diminished in infected samples and support for our chosen approach a of modified TRAP system. RNA samples were then bioanalyzed, yielding RINs from 6 to 9 (table 3) (figure 27). In two samples, the RIN was listed as N/A.

However, samples showed normal peaks and this RIN score may be due to noise or a slightly altered ribosomal ratio. All samples were of good enough quality to send for sequencing.

Table 3. Total amount of RNA and RIN scores for RNA samples extracted via TRAP or total RNA extracted from CLE.

REP CODE	LINE, CONDITION, REPLICATE	TOTAL UG	RIN
PMT 1	419F2 MOCK #4 (TRAP)	7.23	8.3
PMT 2	419F2 MOCK #8 (TRAP)	8.31	8.6
PMT 3	419F2 MOCK #13 (TRAP)	9.57	8.4
PMT 4	419F2 MOCK #14 (TRAP)	10.98	8.5
PMT 5	419F2 MOCK #15 (TRAP)	10.89	8.9
PIT 1	419F2 INF #6 (TRAP)	6.60	8.8
PIT 2	419F2 INF #7 (TRAP)	7.65	8.6
PIT 3	419F2 INF #8 (TRAP)	5.92	9.7
PIT 4	419F2 INF #9 (TRAP)	6.21	9
PIT 5	419F2 INF #10 (TRAP)	6.02	8.9
DIT 1	414C4 INF #7 (TRAP)	1.39	N/A
DIT 2	414C4 INF #8 (TRAP)	1.16	9
DIT 3	414C4 INF #9 (TRAP)	1.76	9.3
DIT 4	414C4 INF #10 (TRAP)	1.25	N/A
DIT 5	414C4 INF #11 (TRAP)	1.20	6.9
PMC 1	419F2 MOCK #4 (CLE)	10.47	6.8
PMC 2	419F2 MOCK #8 (CLE)	11.96	6.7
PMC 3	419F2 MOCK #13 (CLE)	13.24	6.9
PMC 4	419F2 MOCK #14 (CLE)	14.45	7.3
PMC 5	419F2 MOCK #15 (CLE)	11.20	7.3
PIC 1	419F2 INF #6 (CLE)	10.37	7.4
PIC 2	419F2 INF #7 (CLE)	9.98	6.9
PIC 3	419F2 INF #8 (CLE)	10.01	6.5
PIC 4	419F2 INF #9 (CLE)	9.63	6.6
PIC 5	419F2 INF #10 (CLE)	12.39	7.9
DMC 1	414C4 MOCK #6 (CLE)	12.19	7.9
DMC 2	414C4 MOCK #8 (CLE)	10.41	7.8
DMC 3	414C4 MOCK #14 (CLE)	15.34	7.9
DIC 1	414C4 INF #7 (CLE)	11.04	7.8
DIC 2	414C4 INF #8 (CLE)	13.69	7.8
DIC 3	414C4 INF #9 (CLE)	13.77	8.3
DIC 4	414C4 INF #10 (CLE)	13.97	8
DIC 5	414C4 INF #11 (CLE)	12.36	8.2

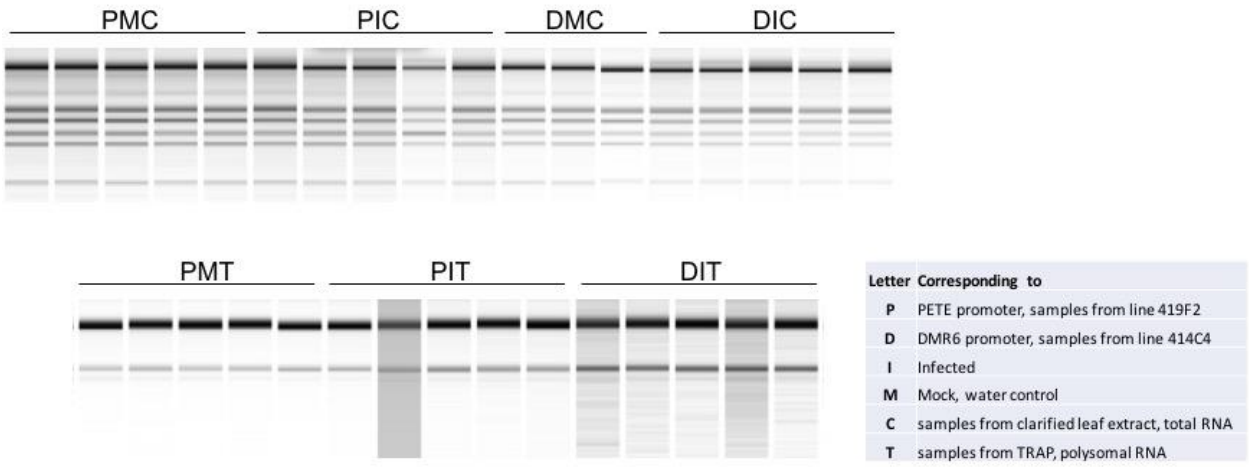

Figure 27. Bioanalyzer results from samples to be sent for sequencing. RNA from clarified leaf extract (denoted by "C") and immunopurified polysomes (denoted by "T") was assayed with an Agilent 2100 Bioanalyzer. Images show presence of in-tact total RNA from CLE samples, ribosomal RNA from immunopurified samples. Each lane corresponds to RNA extracted from separate biological replicates and TRAP extractions of each sample condition.

CHAPTER VI

The TRAP data

TRAP-RNA samples and their total RNA counterparts were sent for paired-end sequencing. Samples were sent with 3-5 biological replicates, as outlined in figure 23, for a total of 30 prepared libraries. Library preparation and sequencing were performed by Mrs. RNA Lab (Mr. DNA Lab, Shallowater, Texas). Libraries were analyzed for sequence quality through FastQC, and reads were trimmed via Trimmomatic prior to alignment [63, 64]. Libraries were mapped to the TAIR10 Col-0 reference genome using STAR, and experimental conditions had variable alignments, from 79% to 96% average uniquely mapped reads (figure 28) [65]. This variability may stem from the experimental design itself- replicates of total RNA from infected samples showed lower percentages of mapped reads due to the presence of *Hpa* RNA within the leaves. Samples of total RNA as well as TRAP RNA from mock-infected samples showed the highest percentage of mapped reads. TRAP RNA from infected samples showed different percentages of mapped reads from the mesophyll samples (92%) and the haustoriated cells samples (87%). This may be due to a greater amount of *Hpa* RNA in DMR6-TRAP samples (as seen in TRAP quality-control qPCR assays, figure 26).

Further analyses remain to be completed for useful, biologically-relevant information to be extracted from this data set.

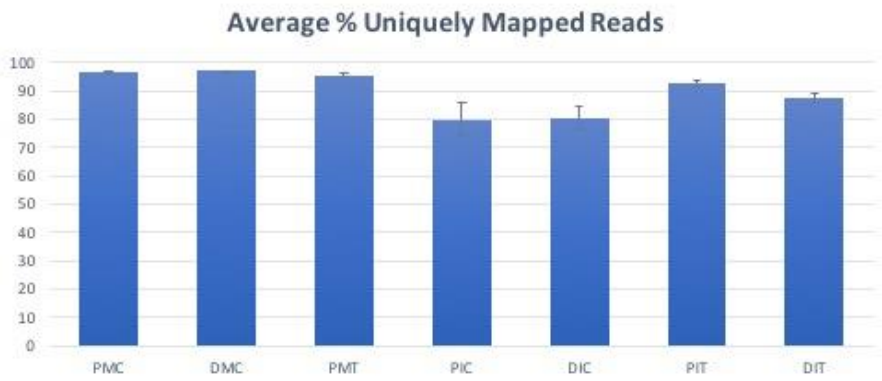

Figure 28. Average percent uniquely mapped reads from different sample conditions. Average percentage of mapped reads from all replicated within a given experimental condition. Samples from total RNA extracted from infected samples (PIC, DIC) show the least percentage of mapped reads and greatest variability of mapped reads between replicates.

CHAPTER VII

The transfer assay

Several examples of transfer of a radio-labeled nutrient from host plant to pathogen have been published. In the case of a downy mildew pathogen, tritium-labeled glucose and leucine were supplied to lettuce cotyledons via petiole uptake, and the cotyledons were subsequently infected with *Bremia lactuca*. Both the plant and the pathogen were then analyzed for radioactivity, and it was found that the oomycete was able to take up radiolabeled compounds from the host plant [66].

In another case, wheat leaves infected with *Erysiphe graminis* f.sp. *tritici* (with the infection primarily contained to the upper epidermis) were placed in radiolabeled sugar solution. The leaves were removed and dried, and the fungus was removed by placing tape over the epidermis and carefully peeling it away with the mycelium remaining on the tape. Plant and pathogen were analyzed via scintillation counting and radioactivity was detectable in pathogen samples [67].

Although the transfer of labeled nutrients has been shown for some plant-pathogen interactions, there is no established or published protocol for *Hpa* on Arabidopsis. Unique challenges exist in our chosen system due to the lifestyle of *Hpa*. We cannot extract the hyphae without major disruption of the leaf, and in order to collect spores the leaves must be treated in a delicate manner leading up to pathogen sporulation. Therefore, there is a need for the creation of a novel transfer assay to show uptake and transfer of labeled amino acids from Arabidopsis to *Hpa*.

To address this need, experiments were performed in an attempt to track tritium-labeled glutamine from Arabidopsis seedlings to *Hpa* spores. The general experimental outline involved infecting Arabidopsis with *Hpa*, transferring cut plants into radio-labeled solution at 6dpi, and inducing sporulation via high humidity overnight. Spores were harvested and both the plants and spores were assayed for radioactive content by scintillation counting (figure 29).

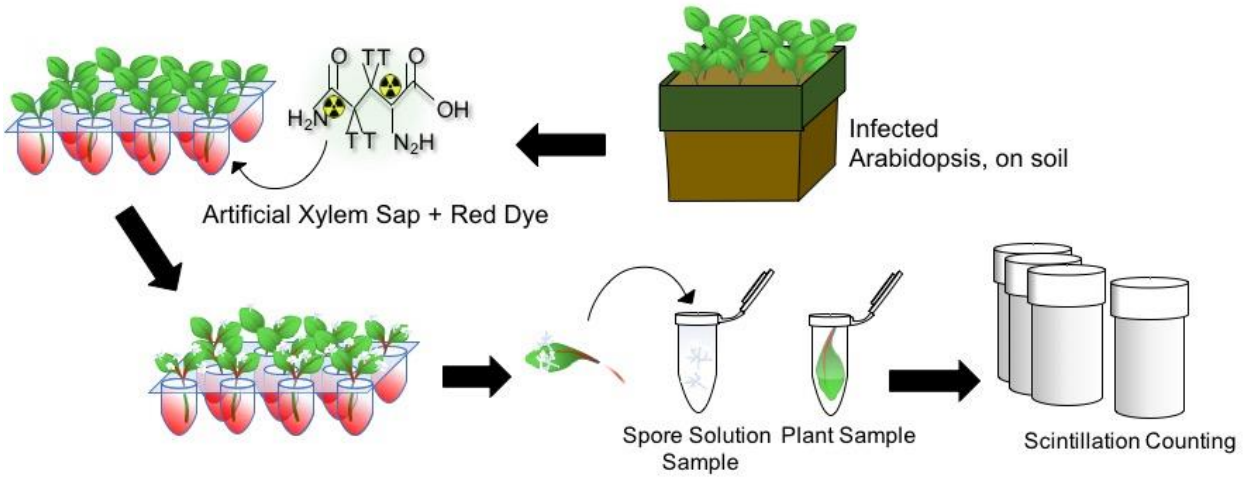

Figure 29. Transfer Assay Experimental Outline. Infected Arabidopsis is cut at the soil line and transferred to wells containing artificial xylem sap, red dye, and tritium labeled glutamine. *Hpa* sporulates overnight under humid conditions. Spore and leaves are harvest separately, and the section of the leaf in contact with the radioactive solution is removed. Both samples are processed for scintillation counting.

The data collected from these experiments yielded no definitive results, in that very few spore samples yielded enough radioactivity to be considered counted about threshold background levels. In addition, most trends for radioactivity in spore samples were inconsistent from replicate to replicate. The only noticeable and repeatable trend was that sporulated plant samples had less radioactivity than infected, non-sporulating samples. In theory, this "lost" radioactivity should be accounted for in the pathogen spores, which are the only part of the oomycete that is not permanently associated with host plant. However, since spore samples did not yield accurately quantifiable levels of radioactivity, conclusions cannot be drawn (figure 30).

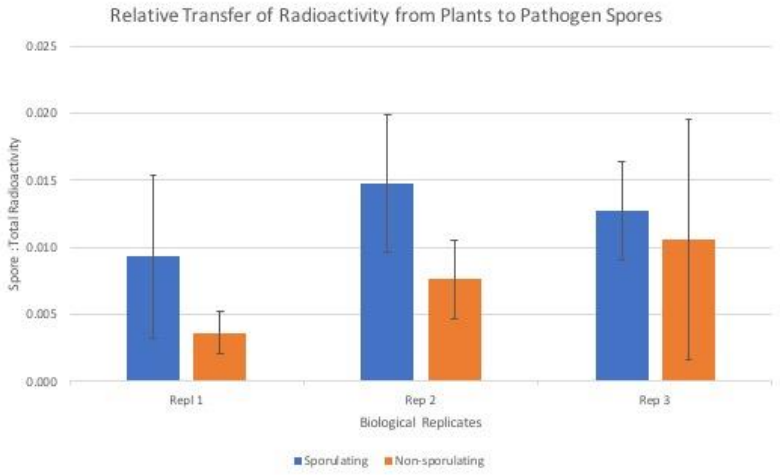

Figure 30. Example of variability between replicates of Transfer Assay Experiment. Large variability is shown between biological replicated, but also within technical replicates.

CHAPTER VIII

Conclusions and future directions

I have created a modified TRAP system using split GFP as a protein linker, allowing for immunopurification of currently translating ribosomes and polysomes with regards to temporal and spatial requirements. This system is advantageous to the classic single-promoter TRAP system because it employs the use of two promoters, allowing for purification of currently translating ribosomes from ephemeral or transient cell types.

The constructs as they were designed allow for a user of this technology to easily clone and use any two promoters of their choosing. For our experiments, we selected pathogen-inducible and tissue-specific promoters to study plant-pathogen interactions. Our specific interest was in gathering genetic information from haustoriated cells. Using the modified TRAP technology, we were able to isolate high-quality translating and total RNA in amounts sufficient for RNA sequencing.

RNA sequencing data will be analyzed to answer several biological questions: Under normal conditions, is there a significant difference in gene expression between the translatome and transcriptome? Is the difference altered during pathogen infection and colonization? Is there a significant difference in gene expression between the translatome of haustoriated cells and that of the mesophyll as a whole? Which genes are significantly different in haustoriated cells? What does the data tell us about nutrient transport in haustoriated cells, and in the mesophyll during infection?

CHAPTER IX

Methods

In-Fusion Multiple Fragment Cloning

Primers were designed for each fragment (piece) with 10-20 bp overlaps corresponding to the fragments that would be adjacent to the amplified fragment in each corresponding clone through VectorNTI software. Fragments were amplified from templates ((gBlocks Gene Fragments (Integrated DNA Technologies, CA, USA), Col-0 genomic DNA, existing fragments) by PCR with KOD DNA polymerase (Toyobo, Osaka, Japan). Amplified fragments were then gel purified with the GeneJET Gel Extraction Kit (Thermo Fisher Scientific, USA) and used for In-Fusion Multiple Fragment Cloning (Clontech, Takara Bio group, Kyoto, Japan) according to manufactures directions. Clones were sequenced through Eton Biosciences (San Diego, CA).

E.coli Transformation

Heat-shock competent TOP10 cells from (Home made in Pilot Lab) were transformed via modified heat shock protocol: samples are incubated with DNA for 15 minutes on ice, 60 seconds at 42C, and incubated with 250 µl SOC for 1 hours with gentle agitation at 37°C. Cell suspension was centrifuged 3000xg for 3min, supernatant is removed, and cells are resuspended in 50 µl SOC and plated on LB medium with the appropriate antibiotic.

Agrobacterium Transformation

Plasmids were purified from E.coli clones were used to transform *Agrobacterium tumefaciens* strain GV3101 through heat shock. DNA was mixed with competent cells and incubated 5 minutes on ice, 5 minutes in liquid nitrogen, and 5 minutes at 37°C. The competent cells are then incubated for 3 hours shaking in 500 µl LB liquid medium at 30°C. The suspension is then spun down at 3500xg for 3 min, and the supernatant is removed. Pelleted cells were resuspended in 250 µl LB medium and plated on LB medium containing rifampicin, gentamycin, and the antibiotic corresponding to appropriate marker.

Fluorescence Microscopy

Leaves were infiltrated with water via syringe or vacuum and placed on slides with abaxial side facing the slide cover. Imaging performed on a Zeiss LSM 880 confocal laser scanning microscope. Imaging was performed using Zen Black software.

Western Blot

Aliquots from different stages of TRAP were prepared with 1 M DTT and 4X NuPAGE LDS sample buffer, denatured at 90°C for 10 min, and analyzed by SDS-PAGE (4-12% polyacrylamide NuPAGE MES gel, Life Technologies). Proteins were transferred on a nitrocellulose membrane (GE Healthcare). The membrane was treated with Ponceau red stain for visualization of protein samples. The membrane was blocked in OneBlock (Genesee Scientific, CA, USA). Proteins were detected using primary antibodies: anti-flag (monoclonal anti-flag M2, Sigma, 1:1000) or anti-cMyc (Clone A-14, Santa Cruz; 1:1,000) and secondary antibody anti-mouse (1:10,000) in OnBlock buffer. Blots were exposed using ECL-Plus western blotting detection system (GE Healthcare), and recorded by ChemiDoc CCD camera imaging system (Biorad, CA, USA).

Arabidopsis thaliana and Nicotiana benthamiana lines and growth

Arabidopsis thaliana and *Nicotiana benthamiana* were grown under 120 µE/m^2/s, 22oC, 16 h light /8 h dark on soil (Sunshine Mix, Sungro Horticulture, MA, USA) and were watered from below with 300 mg/l Miracle-Gro Fertilizer (Scotts, Marysville, OH, USA). Arabidopsis Ecotype Columbia 0 (Col-0) CS70000 was used for all experiments. Arabidopsis thaliana were transformed by the floral dip method using Agrobacterium tumefaciens GV3101 (pMP90) [68].

Transgenic Arabidopsis Seed Sterilization and Selection

Seeds were sterilized with a solution of sodium dichloroisocyanurate in water and ethanol as follows: for 10 ml, 300mg sodium dichloroisocyanurate in 5 ml H2O and 5 ml 100% ethanol. 10-150 µl

seeds were incubated in 1 ml solution, at 1,400 rpm (Eppendorf thermomixer) at 20 ºC. Under a sterile hood, seeds are then washed with 1ml ethanol three times, and allowed to dry overnight. Seeds were plated on ½ MS medium with antibiotics (kanamycin or hygromycin) to select for transformants or for segregation counting. Plated seeds were incubated at 4°C in the dark overnight and placed in either a growth chamber or on bench tops for germination and growth. Seedlings are transferred to soil after 7 days.

Transient expression in Nicotiana Benthamiana

For transient expression of constructs in *N. benthamiana*, leaves of five-week old plants were infiltrated with a suspension of *Agrobacterium tumefaciens* GV3101pMP90 carrying the constructs or p19 [69]. The bacteria were grown overnight in LB medium supplemented with appropriate antibiotics, washed twice in 10 mM $MgCl_2$, 100 µM acetosyringone, and diluted to final OD_{600} of 0.05 in the same solution.

Translating ribosome affinity purification

Translating ribosome affinity purification protocol was followed according to the published protocol from Mustroph et al. with several modifications [38]. For tobacco samples, the protocols for sucrose cushion isolation and flag bead purification were combined. In this modified protocol, 8 ml of extraction buffer was added to 1.5 g of ground tissue. The leaf extract was clarified twice via centrifugation, with a miracloth filtering step between centrifugations. Six ml of clarified leaf extract were loaded on top of the sucrose cushion. The sucrose cushion contained added detergents (DOC, PTE, and Detergent Mix) in the same molar concentrations as the extraction buffer, and the final concentration of sucrose was 1.7M. Instead of resuspension buffer, polysomes were resuspended in 500 µl extraction buffer. Polysome pellets were agitated via spinning wheel at 4°C overnight, and remaining debris that were not resuspended were removed through a brief centrifugation step for 1 min, 8200xg at 4°C. The resuspended polysomes were added to extraction buffer to a final volume of 5 ml with the addition of 100 µl washed flag beads. Polysomes were incubated with the beads for 2 h with gentle rocking at 4°C. Bead washes were as follows: 1 wash with 5ml extraction buffer, 4 washes with 5 ml wash buffer with, 5 min incubation periods between washes. All buffer was removed from beads, and RNA was extracted directly from them using the Bioline plant RNA extraction kit.

For Arabidopsis samples, clarified leaf extract was added directly to washed flag beads, and followed the same incubation and wash protocol as above. To account for a lower number of tagged ribosomes, clarified leaf extract samples from the DMR6-driven flag-GFP line were saved and used for a second consecutive incubation with an additional 100ul of washed flag beads.

Transfer Assay

3-week-old Arabidopsis plants were infected with *Hpa*. At 6 dpi, leaves were cut at the bottom of the petiole and placed into 300 µl H2O. Leaves were then transferred into 300 µl artificial xylem sap, prepared as published and supplemented with tritium-labeled Gln and 1% safranin red dye [70]. Leaves were then placed in containers and returned to the growth chamber. In the evening, the sporulating samples were subjected to increased humidity overnight to induce sporulation. The next day, spores were harvest by pipetting 10 µl of H_2O up and down on leaf surface. Spores were added to 5 ml Ultima

Gold XR Scintillation Cocktail in scintillation vials (Perkin Elmer, Millipore Sigma, USA). Petioles were removed and leaves and placed in empty scintillation vials were dried at 70°C for 2-3 h. 500 µl household bleach (~8.5% NaClO) was added to the leaves and left at room temp in a closed vial overnight. Vials were then opened for one hour, and 5 ml Scintillation Cocktail was added. All samples were mixed by inversion 10-15 times and left to equilibrate for 1 ho in the dark. Samples were counted in an LSC for 4 min per sample.

RNA Extractions

RNA extraction was performed from Arabidopsis tissue, clarified leaf extract, resuspended polysomes, or flag-beads by either 1 ml TRI REAGENT (Sigma-Aldrich) or with the ISOLATE II RNA Plant kit (Bioline, Meridian Life Science, Memphis, TN). RNA integrity was confirmed by either gel electrophoresis or by bioanalyzer using the Agilent 2100 Bioanalyzer instrument, software and preparation kit according to manufacturer instructions (Agilent, Santa Clara, CA).

GUS Staining

GUS staining was performed with fresh leaf tissue. Leaves were harvested into 1 ml phosphate buffer (50 mM, pH 7.2) containing 25% Triton. Leaves were fixed via infiltration and incubation with 500ml phosphate buffer + 4.5% formaldehyde. Fixed leaves were then washed three times in 1ml phosphate buffer with 500 µM potassium ferrocyanide and potassium ferricyanide with 5 minute incubation periods. Washed leaves were then infiltrated with wash buffer as above, containing 1 mM X-Gluc. Samples were incubated with 37C in the dark until staining became visible, and were cleared with ethanol for imaging.

Dexamethasone Induction

Soil grown three-week old plants were sprayed with 50 µM dexamethasone, (dissolved in DMSO before dilution), and 0.03% Vac-In-Stuff (silwet-77) (Momentive Performance Materials, NY, USA) in the final solution. Plants were covered overnight and either used for GUS staining or fluorescence microscopy. For sterilized seed samples, seeds were germinated on plates containing 50 µM dexamethasone in ½ MS medium. Seedlings were used for GUS staining after 7 days.

Trypan Blue Stain

Trypan blue staining of *Hpa* hyphae, haustoria, and spores was used according to published protocols with some modification [71]. Leaves were incubated for 90 seconds at 90°C, incubated at room temperature for 5 min, and de-stained with chloral hydrate.

Infected Plant Nucleic Acid Isolation and Pathogen Quantification via RT-PCR

Infected Arabidopsis tissue was harvested at 6dpi with *Hpa* and ground to a fine powder in liquid nitrogen. DNA was extracted using the BioSprint 96 DNA Plant kit (Qiagen, Hilden, Germany) according to manufacturer's specifications. The protocol as set forth in Anderson et al. was followed with modifications for the use of TaqMan polymerase, reagents, and probes (Applied Biosystems, Foster City, CA) [62].

Quantitative RT-PCR

cDNAs were synthesized from 1.5 µg of RNA using the SuperScript IV Reverse Transcriptase kit (ThermoFisher Scientific, USA) according to manufacturer's instructions in a 10 µl reaction volume. 5 µl of the RT product (diluted 50 times in water), 5 µl of primer mix (1 µM each), and 10 µl of PowerUp SYBR Green Master Mix (Applied Biosystems, Foster City, CA) were mixed and run through the following cycles on the Applied Biosystems 7500 Real-Time PCR System (Thermofisher Scientific, CA, US): 2 min 50°C, 10 min 95°C, 40 times of 15 sec 95°C, 15 sec 55°C, 1 min 72°C.

Hpa Propagation and infection

Hpa isolate NoCo was used for all experiments. Sporangiospore suspensions of 5×10^4 spores/mL were prepared in water from sporulating plants. Spores were applied via Preval™ spray unit (Preval, Inc., Coal City, IL) to 3-week-old Arabidopsis leaves. Inoculated plants were covered overnight, and then uncovered and kept under short-day conditions. Infected plants were covered and the humidity was raised increased to trigger sporulation at 6dpi.

Phytophthora capsici propagation and infection

Phytophthora capsici strain 263 was grown via mycelial plug transfer on V8 medium plates for 7 days in the dark at room temperature. For plant infection, mycelial plugs were transferred to the leaf surface with a droplet of water. Plants were covered for two days to increase humidity, and infection was assayed by fluorescent microscopy at three and five dpi.

REFERENCES

1. Foley, J.A., et al., *Global Consequences of Land Use.* Science, 2005. **309**(5734): p. 570.
2. J. F, G., M. K. C, and N. P, *The economic impact of potato late blight on US growers.* Potato Research, 2001(2): p. 121.
3. Filippi, M.C.C., et al., *Leaf blast (Magnaporthe oryzae) suppression and growth promotion by rhizobacteria on aerobic rice in Brazil.* Biological Control, 2011. **58**(2): p. 160-166.
4. Bardin, M., et al., *Is the efficacy of biological control against plant diseases likely to be more durable than that of chemical pesticides?* Frontiers in Plant Science, 2015. **6**(566).
5. Kemen, E. and J.D.G. Jones, *Obligate biotroph parasitism: can we link genomes to lifestyles?* Trends in Plant Science, 2012. **17**(8): p. 448-457.
6. Coates, M.E. and J.L. Beynon, *Hyaloperonospora arabidopsidis as a Pathogen Model.* Annual Review of Phytopathology, 2010. **48**(1): p. 329-345.
7. Judelson, H., *Metabolic Diversity and Novelties in the Oomycetes.* Annual Review of Microbiology, 2017: p. 21.
8. Mims, C.W., et al., *Ultrastructure of the host-pathogen interface in Arabidopsis thaliana leaves infected by the downy mildew Hyaloperonospora parasitica.* Canadian Journal of Botany, 2004. **82**(7): p. 1001-1008.
9. Lu, Y.J., et al., *Patterns of plant subcellular responses to successful oomycete infections reveal differences in host cell reprogramming and endocytic trafficking.* Cellular Microbiology, 2012. **14**(5): p. 682-697.

10. Caillaud, M.-C., et al., *A downy mildew effector attenuates salicylic acid-triggered immunity in Arabidopsis by interacting with the host mediator complex.* PLoS biology, 2013. **11**(12): p. e1001732.
11. Johnson, R., *Genetic Background of Durable Resistance*, in *Durable Resistance in Crops*, F. Lamberti, J.M. Waller, and N.A. Van der Graaff, Editors. 1983, Springer New York: Boston, MA. p. 5-26.
12. Yamada, K., et al., *Regulation of sugar transporter activity for antibacterial defense in <em>Arabidopsis</em&gt.* Science, 2016. **354**(6318): p. 1427.
13. Baxter, L., et al., *Signatures of Adaptation to Obligate Biotrophy in the Hyaloperonospora arabidopsidis Genome.* Science, 2010. **330**(6010): p. 1549-1551.
14. Wicker, T., et al., *The wheat powdery mildew genome shows the unique evolution of an obligate biotroph.* Nature genetics, 2013. **45**(9): p. 1092.
15. Kemen, E., et al., *Gene gain and loss during evolution of obligate parasitism in the white rust pathogen of Arabidopsis thaliana.* PLoS biology, 2011. **9**(7): p. e1001094.
16. Spanu, P.D., et al., *Genome Expansion and Gene Loss in Powdery Mildew Fungi Reveal Tradeoffs in Extreme Parasitism.* Science, 2010. **330**(6010): p. 1543-1546.
17. Struck, C., *Amino acid uptake in rust fungi.* Frontiers in plant science, 2015. **6**: p. 40.
18. Chen, L.-Q., et al., *Transport of sugars.* Annual review of biochemistry, 2015. **84**: p. 865.
19. Lalonde, S., D. Wipf, and W.B. Frommer, *Transport mechanisms for organic forms of carbon and nitrogen between source and sink.* Annual review of plant biology, 2004. **55**(1): p. 341-372.
20. Hartung, M.L., et al., *Sugar transporters for intercellular exchange and nutrition of pathogens.* Nature, 2010. **468**(7323): p. 527-532.
21. Chen, H.Y., et al., *The Arabidopsis vacuolar sugar transporter SWEET2 limits carbon sequestration from roots and restricts Pythium infection.* The Plant Journal, 2015. **83**(6): p. 1046-1058.
22. *BIOCHEMISTRY & MOLECULAR BIOLOGY OF PLANTS*. Vol. 2ND. 2015, CHICHESTER: WILEY-BLACKWELL.
23. Chen, L. and D.R. Bush, *LHT1, A Lysine- and Histidine-Specific Amino Acid Transporter in Arabidopsis.* Plant Physiology, 1997. **115**(3): p. 1127.
24. Hirner, A., et al., *Arabidopsis LHT1 Is a High-Affinity Transporter for Cellular Amino Acid Uptake in Both Root Epidermis and Leaf Mesophyll.* The Plant Cell, 2006. **18**(8): p. 1931-1946.
25. Liu, G., et al., *Amino acid homeostasis modulates salicylic acid-associated redox status and defense responses in Arabidopsis.* The Plant Cell, 2010. **22**(11): p. 3845-3863.
26. Shin, K., et al., *Genetic Identification of ACC-RESISTANT2 Reveals Involvement of LYSINE HISTIDINE TRANSPORTER1 in the Uptake of 1-Aminocyclopropane-1-Carboxylic Acid in Arabidopsis thaliana.* Plant and Cell Physiology, 2015. **56**(3): p. 572-582.
27. Pratelli, R. and G. Pilot, *Altered amino acid metabolism in glutamine dumper1 plants.* Plant Signaling and Behavior, 2007. **2**(3): p. 182-184.
28. Pilot, G., et al., *Overexpression of GLUTAMINE DUMPER1 leads to hypersecretion of glutamine from hydathodes of Arabidopsis leaves.* The Plant Cell, 2004. **16**(7): p. 1827-1840.
29. Yang, H., et al., *Altered growth and improved resistance of Arabidopsis against Pseudomonas syringae by overexpression of the basic amino acid transporter AtCAT1.* Plant, Cell and Environment, 2014. **37**(6): p. 1404-14.
30. Yang, H. and U. Ludewig, *Lysine catabolism, amino acid transport, and systemic acquired resistance: What is the link?* plant Signaling and Behavior, 2014. **9**.
31. Qiaona, P., et al., *RTP1 encodes a novel endoplasmic reticulum (ER)-localized protein in Arabidopsis and negatively regulates resistance against biotrophic pathogens.* New Phytologist, 2016. **209**(4): p. 1641-1654.

32. Müller, B., et al., *Amino Acid Export in Developing Arabidopsis Seeds Depends on UmamiT Facilitators.* Current Biology, 2015. **25**(23): p. 3126-3131.
33. Fend, F. and M. Raffeld, *Laser capture microdissection in pathology.* Journal of clinical pathology, 2000. **53**(9): p. 666-672.
34. Bonner, W.A., et al., *Fluorescence Activated Cell Sorting.* Review of Scientific Instruments, 1972. **43**(3): p. 404-409.
35. Nakazono, M., et al., *Laser-Capture Microdissection, a Tool for the Global Analysis of Gene Expression in Specific Plant Cell Types: Identification of Genes Expressed Differentially in Epidermal Cells or Vascular Tissues of Maize.* The Plant Cell, 2003. **15**(3): p. 583-596.
36. Richardson, G.M., J. Lannigan, and I.G. Macara, *Does FACS perturb gene expression?* Cytometry Part A, 2015. **87**(2): p. 166-175.
37. Heiman, M., et al., *A Translational Profiling Approach for the Molecular Characterization of CNS Cell Types.* Cell, 2008. **135**(4): p. 738-748.
38. Mustroph, A., P. Juntawong, and J. Bailey-Serres, *Isolation of plant polysomal mRNA by differential centrifugation and ribosome immunopurification methods.* Methods in molecular biology 2009. **553**: p. 109.
39. Zanetti, M.E., et al., *Immunopurification of Polyribosomal Complexes of Arabidopsis for Global Analysis of Gene Expression.* Plant Physiology, 2005. **138**(2): p. 624-635.
40. Adams, J.U., *Transcriptome: Connecting the Genome to Gene Function*, in *Nature Education*. 2008, Nature. p. 195.
41. Wang, T., et al., *Translating mRNAs strongly correlate to proteins in a multivariate manner and their translation ratios are phenotype specific.* Nucleic acids research, 2013. **41**(9): p. 4743-4754.
42. Halbeisen, R.E. and A.P. Gerber, *Stress-dependent coordination of transcriptome and translatome in yeast.* PLoS biology, 2009. **7**(5): p. e1000105.
43. Meteignier, L.-V., et al., *Translatome analysis of an NB-LRR immune response identifies important contributors to plant immunity in Arabidopsis.* Journal of Experimental Botany, 2017. **68**(9): p. 2333-2344.
44. Mustroph, A., et al., *Profiling Translatomes of Discrete Cell Populations Resolves Altered Cellular Priorities during Hypoxia in Arabidopsis.* Proceedings of the National Academy of Sciences of the United States of America, 2009. **106**(44): p. 18843-18848.
45. Van Damme, M., et al., *Arabidopsis DMR6 encodes a putative 2OG-Fe(II) oxygenase that is defense-associated but required for susceptibility to downy mildew.* The Plant Journal, 2008. **54**(5): p. 785-793.
46. Martin, C., *GREEN FLUORESCENT PROTEIN.* Photochemistry and Photobiology, 1995. **62**(4): p. 651-656.
47. Ito, M., T. Ozawa, and S. Takada, *Folding Coupled with Assembly in Split Green Fluorescent Proteins Studied by Structure-based Molecular Simulations.* The Journal of Physical Chemistry B, 2013. **117**(42): p. 13212-13218.
48. Pedelacq, J.-D., et al., *Engineering and characterization of a superfolder green fluorescent protein.* Nature Biotechnology, 2006(1).
49. Cabantous, S., et al., *A new protein-protein interaction sensor based on tripartite split-GFP association.* Scientific Reports, 2013. **3**: p. 2854-2854.
50. Gallie, D.R., *The 5'-leader of tobacco mosaic virus promotes translation through enhanced recruitment of eIF4F.* Nucleic Acids Research, 2002. **30**(15): p. 3401-3411.
51. Purcell, O., J. Peccoud, and T.K. Lu, *Rule-based design of synthetic transcription factors in eukaryotes.* ACS synthetic biology, 2014. **3**(10): p. 737-744.
52. Goodin, M.M., et al., *Nicotiana benthamiana: Its History and Future as a Model for Plant-Pathogen Interactions.* Molecular Plant-Microbe Interactions: MPMI, 2015. **2015**(1): p. 28-39.

53. Schroeder, A., et al., *The RIN: an RNA integrity number for assigning integrity values to RNA measurements.* BMC Molecular Biology, 2006. **7**: p. 3-3.
54. Takashi, A. and C. Nam-Hai, *A glucocorticoid-mediated transcriptional induction system in transgenic plants.* The Plant Journal, 1997. **11**(3): p. 605-612.
55. Kay, R., et al., *Duplication of CaMV 35S Promoter Sequences Creates a Strong Enhancer for Plant Genes.* Science, 1987. **236**(4806): p. 1299-1302.
56. Berardini Tanya, Z., et al., *The arabidopsis information resource: Making and mining the "gold standard" annotated reference plant genome.* genesis, 2015. **53**(8): p. 474-485.
57. Ishida, H., et al., *Mobilization of Rubisco and Stroma-Localized Fluorescent Proteins of Chloroplasts to the Vacuole by an ATG Gene-Dependent Autophagic Process.* Plant Physiology, 2008. **148**(1): p. 142-155.
58. Lebel, E., et al., *Functional analysis of regulatory sequences controllingPR-1 gene expression in Arabidopsis.* The Plant Journal, 2001. **16**(2): p. 223-233.
59. Zeilmaker, T., et al., *DOWNY MILDEW RESISTANT 6 and DMR6-LIKE OXYGENASE 1 are partially redundant but distinct suppressors of immunity in Arabidopsis.* Plant Journal, 2015. **81**(2): p. 210-222.
60. Ah-Fong, A.M.V. and H.S. Judelson, *Vectors for fluorescent protein tagging in Phytophthora: tools for functional genomics and cell biology.* Fungal Biology, 2011. **115**(9): p. 882-890.
61. Hily, J.-M., et al., *A transformation booster sequence (TBS) from Petunia hybrida functions as an enhancer-blocking insulator in Arabidopsis thaliana.* Plant Cell Reports, 2009. **28**(7): p. 1095-1104.
62. G., A.R. and M.J. M., *A PCR assay for the quantification of growth of the oomycete pathogen Hyaloperonospora arabidopsidis in Arabidopsis thaliana.* Molecular Plant Pathology, 2015. **16**(8): p. 893-898.
63. Andrews, S., *FastQC A Quality Control tool for High Throughput Sequence Data.* http://www.bioinformatics.babraham.ac.uk/projects/fastqc/.
64. Bolger, A.M., M. Lohse, and B. Usadel, *Trimmomatic: a flexible trimmer for Illumina sequence data.* Bioinformatics, 2014. **30**(15): p. 2114-2120.
65. Dobin, A., et al., *STAR: ultrafast universal RNA-seq aligner.* Bioinformatics, 2013. **29**(1): p. 15-21.
66. Andrews, J.H., *Distribution of label from 3H-glucose and 3H-leucine in lettuce cotyledons during the early stages of infection with Bremia lactucae.* Canadian Journal of Botany, 1975. **53**(11): p. 1103-1115.
67. Sutton, P.N., M.J. Henry, and J.L. Hall, *Glucose, and not sucrose, is transported from wheat to wheat powdery mildew.* Planta, 1999. **208**(3): p. 426-430.
68. Clough Steven, J. and F. Bent Andrew, *Floral dip: a simplified method for Agrobacterium - mediated transformation of Arabidopsis thaliana.* The Plant Journal, 2008. **16**(6): p. 735-743.
69. Voinnet, O., et al., *Retracted: An enhanced transient expression system in plants based on suppression of gene silencing by the p19 protein of tomato bushy stunt virus.* The Plant Journal, 2003. **33**(5): p. 949-956.
70. Wilkinson, S., et al., *Effects of Xylem pH on Transpiration from Wild-Type and flacca Tomato Leaves : A Vital Role for Abscisic Acid in Preventing Excessive Water Loss Even from Well-Watered Plants.* Plant Physiology, 1998. **117**(2): p. 703-709.
71. van Wees, S., *Phenotypic Analysis of Arabidopsis Mutants: Trypan Blue Stain for Fungi, Oomycetes, and Dead Plant Cells.* Cold Spring Harbor Protocols, 2008. **2008**(8): p. pdb.prot4982.